NEW YORK UNIVERSITY

College of Engineering
RESEARCH DIVISION
University Heights, New York 53, N. Y.

SOME INVESTIGATIONS OF MOLECULAR SPECTRA AT DECIMETER WAVELENGTHS

Report No. 195.2
October 31, 1953

Low Frequency Microwave Spectroscopy Project

Prepared for
Electronics Branch
Office of Naval Research
Washington, D.C.
Contract No. Nonr 621 (00)

SOME INVESTIGATIONS OF MOLECULAR SPECTRA AT DECIMETER WAVELENGTHS

Report No. 195.2

October 31, 1953

Low Frequency Microwave Spectroscopy Project

Prepared by: Yardley Beers
Yardley Beers
Project Director

Samuel Weisbaum
Samuel Weisbaum

Gabriel Herrmann
Gabriel Herrmann

Fred Sterzer
Fred Sterzer

Approved by: Harold K Work
Harold K. Work
Director of the Research Division

Office of Naval Research

Contract No. Nonr 621 (00)

TABLE OF CONTENTS

FOREWORD

An abstract of this work in conventional form can be found in Section I-B, "Summary of Work Performed", starting on Page 3.

This is the final report on work performed under Contract Nonr 621 (00). Unless otherwise stated specifically, the subject matter represents the status of the work exactly as of the termination date, October 31, 1953.

Since many aspects of this work are being continued, or even expanded, none of this should be considered as complete.

A few brief references will be made to work performed after October 31, 1953, while the writing of this report was in progress. Such work was performed while under contract with the United States Air Forces through the Office of Scientific Research, Contract No. AF 18 (600) 698. Details of such work will be described ultimately in reports issued under that contract.

I. INTRODUCTION

A. Objective

The purpose of this project has been to extend the observations of absorption spectra of gases and vapors to frequencies considerably lower than those conventionally employed in microwave spectroscopy. Previously very little work had been done at frequencies below the X-band, that is below 9000 Mc/sec, because intensities of absorption lines tend to decrease rapidly with a decrease in frequency and because simple molecules, whose spectra are easy to analyze, generally do not have any lines in the lower frequency region. The only previously published papers dealing with spectra below 3000 Mc/sec concern two molecules, heavy ammonia (ND_3)[1] and bromoform ($CHBr_3$).[2] Nevertheless there are many more molecules which may be expected to have spectra in this region, and our calculations and experiments have shown that intensities are sufficient for practical work at frequencies still lower than those employed in the work on ND_3 and $CHBr_3$. In the low frequency region it is possible to obtain many data which can be very valuable in contributing to an analysis of the spectra of molecules of complex structure. Furthermore the discovery of lines of appreciable intensity can be useful for practical applications such as frequency standards and filters.

The spectra which are observable in the lower frequency region generally have the same origin as those in the higher frequency regions. The principal type is due to rotational transitions

in the molecules, but other types can be observed. Symmetrical top molecules, if they have rotational transitions at low frequencies, are heavy molecules, whose spectra generally have complicated hyperfine splittings. The lowest rotational transitions, which are the ones which occur at low frequencies, are the ones which have the simplest hyperfine structure and which yield the most accurate values of the rotational constants because of the small centrifugal distortion effects.

Investigation of very asymmetrical top molecules in this region also may yield useful information. Many lines must be measured to obtain sufficient data for evaluation of the large number of structural constants of these molecules. At the same time, the lines may fall at very scattered frequencies so that an inadequate number may lie in the conventional microwave region. In these cases the data obtained in the lower frequency region may be an invaluable supplement.

In addition to the conventional types of spectra there is the possibility of observing a type peculiar to this region: that due to the recrientation of a nucleus with a large quadrupole moment with respect to a constant rotational angular momentum vector --- the so-called "pure quadrupole" spectra. Such spectra have been observed in solids but no work had been done with vapors. The observation of such spectra should yield more accurate determinations of quadrupole constants than observations on rotational spectra.

B. Summary of Work Performed

A Stark-modulated waveguide microwave spectrometer has been built and operated in the range from 2,150 to 5,000 Mc/sec with a minimum detectable absorption coefficient of about 1×10^{-10} $cm.^{-1}$ Except for the low frequency, this spectrometer is of conventional design. More recently this apparatus has been modified to operate also in the range from 400 to 850 Mc/sec by operating the absorption cell as a transmission line in a TEM mode instead of as a waveguide in the TE_{01} mode. It should be a simple matter to extend the range of this apparatus to adjacent regions.

The spectra of three molecules are being investigated. The work on the very asymmetrical top molecule half-heavy water (HDO) is nearly complete. One P-branch and five Q-branch lines have been completely measured and identified. These data have contributed materially to an evaluation of the structural constants of the molecule. From the data obtained by this and other microwave spectroscopy projects we have computed the principal moments of inertia respectively as having the values of 1.1982, 3.0862, and 4.3887 in units of gm $cm^2 \times 10^{-40}$. In addition the shape of the $3_2 \rightarrow 3_3$ line at 824.64 Mc/sec has been extensively studied. At low pressure the wings of the line have been shown to be wider than is consistent with the Lorentz line shape probably due to the presence of sattelite lines arising from the hyperfine splitting of the energy levels by the quadrupole moment of the deuteron. The observed effects are consistent with a quadrupole coupling constant of 272 ± 90 kc/sec with respect to an axis along the O-D bond.

Investigation of the J = 0 to J = 1 spectrum of the symmetrical top molecule bromoform ($CHBr_3$) is in progress. This transition has a very complicated hyperfine structure because of (a) presence of four isotopic species of the molecule and (b) the presence in each of these of three bromine nuclei each with a nuclear spin of 3/2. To date about twenty lines have been observed between 2275 and 2700 Mc/sec, but none of these has been identified, nor has it been verified that they originate from bromoform rather than from some contaminating vapor.

Work on pure quadrupole spectra of vapors has also been started. According to theory, electric dipole transitions of this type are forbidden for linear molecules in their ground vibrational state but they are allowed for non-linear symmetrical top molecules provided K is not equal to zero. Several transitions of methyl iodide (CH_3I) have been calculated to fall in the vicinity of 500 Mc/sec with intensities sufficient for observation provided that the apparatus is adjusted for the maximum available sensitivity. Experimental work will commence on completion of certain minor modifications of the apparatus necessary for realization of the available sensitivity.*

17
15

C. A Discussion of Experimental Problems

From the point of view of detached analysis, the decreasing intensity of absorption lines with lower frequencies is a fundamental experimental problem. However, except on a few

---

* Note added in proof. Since the above was written, three lines of the quadrupole spectrum of methyl iodide have been observed. See Page 53.

occasions, this problem has seemed very remote to us in the daily operation of the apparatus. In fact, without employing unusual precautions or techniques we have found the sensitivity of the apparatus quite adequate for the work that has been undertaken. To be sure, the decrease in intensity is in a small way compensated by the increase in sensitivity at low frequencies. In general, tubes and crystal detectors produce less noise. In addition, if wave guide absorption cells are employed, the cut-off condition requires these to be of large cross-section. At high pressures these large cells contain for any given length a relatively large number of gas molecules, and the sensitivity may be enhanced by the use of high power levels without danger of power saturation. On the other hand, at reduced pressure smaller line width and greater resolution are obtainable.

There are, however, other experimental problems which have seemed of immediate importance. First there is the matter of spurious lines, which in part is due to the high absolute sensitivity. Many of these appear to be true absorption lines on contaminating gases, while a few appear to be purely of electrical origin. Probably much greater time has been devoted to disproving spurious lines than to verifying genuine ones. Also for a while, one genuine line was hidden by a spurious effect arising from a resonance in the rf system.

One spurious line, apparantly at 2,856 Mc/sec, was found to have a very unusual origin. It was shown to be the strong

$4_1 \rightarrow 4_2$ line of HDO at 5,702 Mc/sec excited by the second harmonic of the klystron. This incident has suggested a difficulty that may arise in work with symmetrical top molecules since the $J = 1$ to $J = 2$ spectrum may be expected to lie in the frequency band which is just the second harmonic of that occupied by the $J = 0$ to $J = 1$ spectrum. Thus if the former should be excited in this spurious manner, it would be hard to indentify the lines properly.

Other serious problems are the related ones of absorption on the walls, pressure stability, and pumping speed. These problems are aggravated by the use of absorption cells of as large cross-section as have been used on this project. Furthermore, if the small line width and high resolution possible with these cells is to be realized, the pressure must be lower than that used in the smaller cells which are employed at higher frequencies.

These problems may be illustrated by the fact that it takes at least three hours of continuous pumping with a diffusion pump to cause a strong HDO line to disappear and that only a short time after the pump has been shut off the line will reappear.

In the region below 1000 Mc/sec there is the additional problem of the narrow bandwidth of the rf system. This impedes search work and in some types of experiment may give undesired distortion of line shapes. In fact in this region usually we have not been able to observe an unsplit line and its Stark components without retuning, and much of the search work is done by using a fixed

frequency near to the predicted frequency of an absorption line and varying the Stark voltage, and thus the Stark components are brought one by one to the operating frequency.

Another problem which arises in this region below 1000 Mc/sec is the decoupling of the rf signal at the detector from the Stark modulation voltage. This difficulty results from the fact that here the absorption cell is operated as a transmission line in a TEM mode with the rf voltage applied to the Stark septum. The residual Stark voltage demodulated by the detector is particularly troublesome in the measurements made with fixed frequency and variable voltage since it causes a variation in the base line of the record.

II. APPARATUS

A. General Design

The spectrometer will be described from the point of view of operation in the S-band, as originally intended. The modifications and special procedures for operation in the uhf region (below 1000 Mc/sec) will be discussed in a special section, number III-G, starting on Page 20.

The spectrometer employs a rectangular S-band waveguide absorption cell with square wave Stark modulation. A block diagram is shown in Figure 1. It is completely conventional in design except for the details resulting from its comparatively low frequency. Except for the absorption cell itself, the entire rf circuit employs flexible coaxial lines for connections. Indirectly because of the low operating frequency an unusually low Stark modulation frequency of 5000 cps is employed.

The choice of Stark frequency is based upon a compromise between three factors favoring the use of a low frequency and two factors favoring a high frequency. The principal reason for favoring a low frequency is to avoid spoiling the resolution since lines are artificially broadened when the Stark modulation frequency becomes comparable to the natural line width. With HDO at room temperature in the present absorption cells, a natural line width due to collisions with the walls and the Doppler effect of about 15 Kc/sec is to be expected, and smaller values are to be expected with

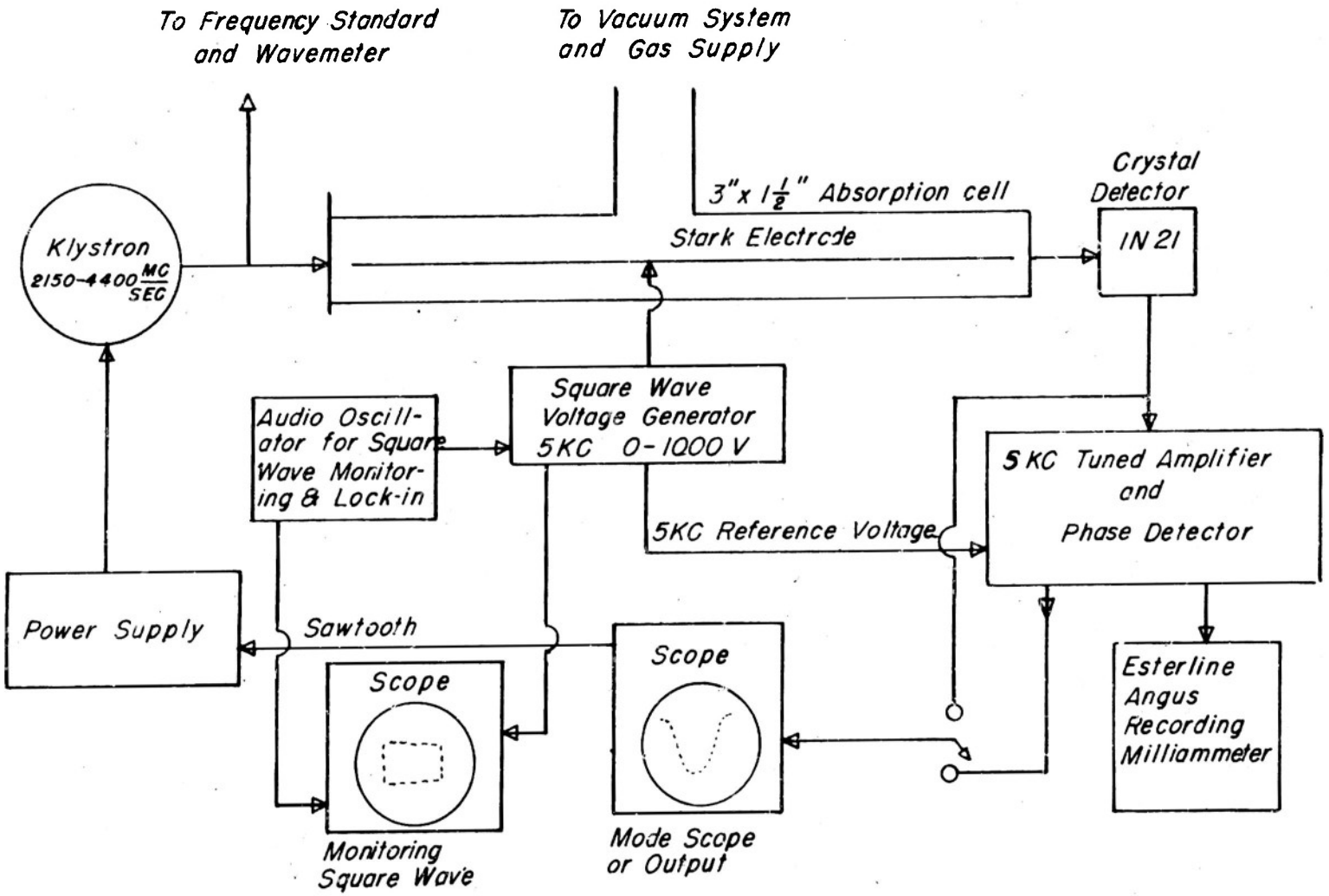

FIG. 1 S-band Stark-Modulated Spectograph

heavier molecules. These natural line widths are smaller than those generally obtained at higher frequencies partly because a larger absorption cell is used and partly because the Doppler broadening is proportional to the frequency of the line. This consideration appeared to be the most important and was the main reason for the selection of 5,000 cps as the modulation frequency.

A minor consideration favoring the use of low frequency is that direct pick-up of the Stark voltage by the detector is smaller. A second minor consideration is that since the current drawn by the final amplifier tubes is proportional to the frequency it is difficult, or at least expensive, to generate high voltages at high frequencies.

The principal reason favoring the use of a high modulation frequency is to reduce noise since the small shot noise produced by the oscillator and the crystal detector varies inversely with the frequency. However, we wonder whether undue importance has been given to this consideration since the decrease of the noise with frequency is to some extent compensated by the fact that generally the noise bandwidth of the amplifier following the detector generally tends to increase with the frequency. A second reason for selecting a high frequency is to make it possible to design an amplifier which will discriminate in favor of the modulation frequency and against power supply ripple frequencies. This requirement is already fulfilled with a frequency as high as 5000 cps.

It might be questioned whether the use of large absorption cells requires an exorbitant amount of Stark voltage since the splitting depends primarily upon the field strength rather than on the voltage. However, with the large absorption cells smaller line widths are obtainable and the same degree of resolution of Stark components can be obtained at proportionally lower field strengths. What is even more important, the Stark coefficients of low frequency lines are generally very large because of the smallness of the so-called "energy denominator" in the lead term of the perturbation calculation of the coefficient. Therefore a square wave generator giving voltages up to 1000 or 1500 volts appears adequate for most purposes.

The intensities of the lines have not been sufficient for presentation on a cathode-ray oscilloscope in the conventional manner employing a saw-toothed sweep with a frequency of the order of 10 cps. Almost throughout a phase-sensitive detector and a recording milliameter have been used. However, on occasion a cathode-ray oscilloscope has been used with Lissajous presentation. The vertical input is connected to the output of the tuned amplifier preceding the phase-sensitive detector, and the horizontal input is connected to the sine wave voltage which is used to synchronize the frequency of the Stark voltage generator. As the frequency of the klystron is slowly varied through an absorption line, the 1:1 Lissajous pattern may be seen to appear and then disappear. This method is improved by the use of a cathode-ray tube with a long persistent screen.

B. Oscillaters

Most of the work has employed 707 "McNally Tube" klystron tubes with a series of cavities operating between from 2150 to slightly beyond 3000 Mc/sec. Some of these cavities were obtained from war surplus while others are of own construction. At higher frequencies the 726A, 2K29, and 2K56 integral cavity tubes have been used. Recently 6BL6 and 6BM6 tubes have been obtained, and a wide band cavity has been constructed for the range 1500 to 6000 Mc/sec, but tests have not been completed, and these tubes have not been used with the spectrometer.

The tubes are subject to magnetic pick-up of power line frequency and mechanical vibrations. Therefore it has been necessary to house them in a steel shock-mounted box. This permits magnetic shielding from the magnetic fields of power transformers and other equipment. To reduce frequency modulation resulting from power supply ripple, two extra sections of RC filter in both the reflector and cavity supply leads have been installed in this box. Also the heater power is supplied from a storage battery. Mainly to assist in tune-up operations, a connector and decoupling network are provided so that a saw-toothed voltage, derived from a cathode-ray oscillescope, may be applied to the reflector.

The power supply provides a cavity voltage variable up to 350 volts and a reflector voltage variable from zero to 150 volts. Occasionally it is necessary to augment the reflecter

voltage by a small battery placed in the box with the klystron. The circuit is one designed by L. M. Belleville[3] except that provision is made for grounding the positive high voltage (that is, the cavity). The slow sweep required for use with the phase-sensitive detector is produced by connecting a slow speed electric motor to the shaft of the potentiometer controlling reflector voltage. In the final measurements of the frequency of a line, some of the readings are made with a 1:1 reversing gear between the motor and the potentiometer, and the value obtained with the frequency increasing is averaged with the value obtained with the frequency decreasing to eliminate errors due to the slow response of the system.

A circuit for stabilizing the frequency of the klystron to the secondary frequency standard, similar to that of Lee et al.[4], has been installed but seldom has been used. The frequencies of the klystron and of a harmonic of the crystal oscillator in the standard are connected to a silicon crystal mixer, whose output is connected to a Hallicrafters SX-63 radio receiver. This is tuned to the desired difference frequency. The dc voltage developed by the FM discriminator then may be used as an error voltage. This voltage is applied to the oscillator through a dc amplifier. The polarity is such as to cause the actual difference frequency to tend to be equal to that of the receiver. The circuit of the 6Y6 dc amplifier is shown in Figure 2. S_2 is thrown in the downward position for the adjustment of the voltage controls on the power supply (which

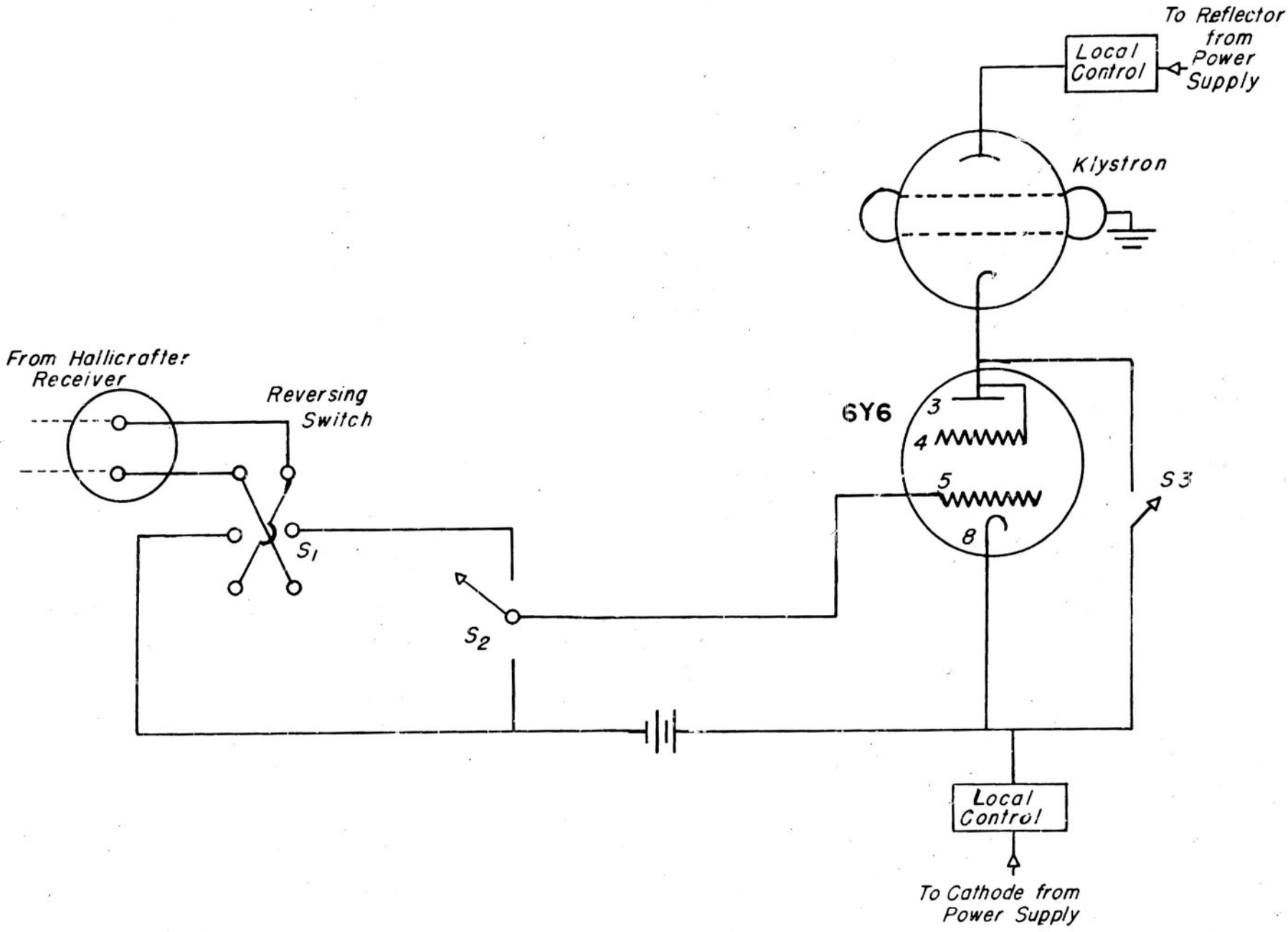

FIG. 2 Stabilization Circuit

are denoted as "local controls") so that the tube is operating in the center of a mode. Then S_2 is thrown into the upward position, and the reversing switch S_1 is thrown into whichever position gives the correct polarity for stabilization. Unfortunately, in one of the positions of S_1, the af amplifier of the receiver is short circuited at the input and monitoring is more difficult. However, by choosing a difference frequency of the correct sign, it is possible to obtain stabilization with the position of S_1 which allows the af amplifier to operate. The heater voltage of the 6Y6 is derived from the same storage battery which supplies the klystron. During adjustment and operation of the stabilizing circuit S_3 is left open. For completely unstabilized operation, S_3 is closed, and the 6Y6 may be removed from its socket to reduce drain on the storage battery.

The required modifications of the SX-63 receiver partially are indicated in Figure 3. The principal objective of these modifications is to insulate the discriminator from ground so that its dc level may be determined by the klystron circuit. All of the original grounds (including one inside the discriminator transformer) are disconnected. The 6H6 dual diode is replaced by two 1N34 crystals mounted on an octal tube base and plugged into the 6H6 socket so that the discriminator is independent of the heater supply of the receiver and thereby is less susceptible to A.C. pick-up. Probably the operation could be improved by "delimitizing" the limiter of the receiver, but this modification has not been incorporated.

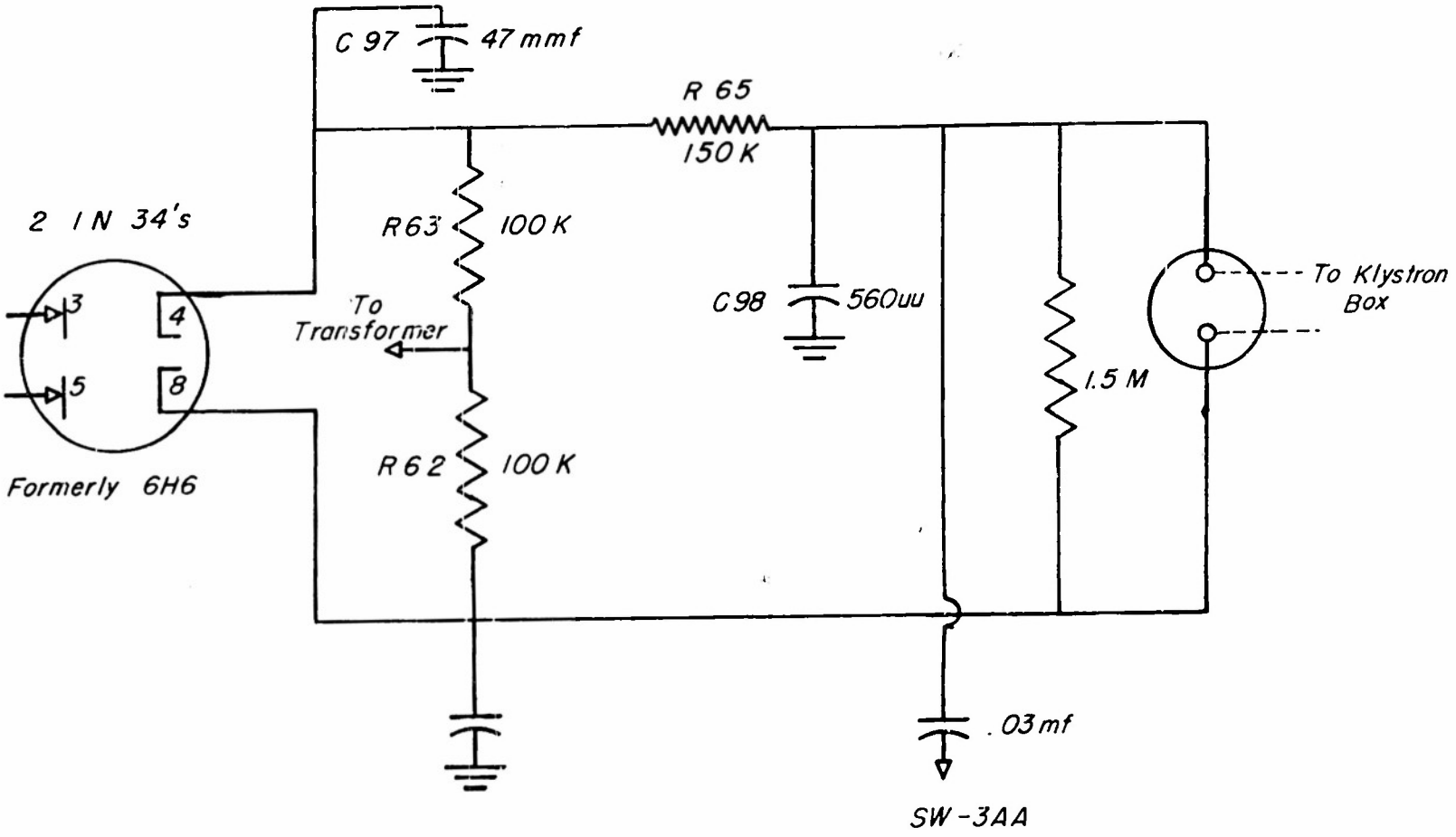

FIG. 3 Modified Discriminator of Hallicrafter Receiver

If a high power level is used in the waveguide, stabilization will hold as the frequency of the receiver is varied through about 4 Mc/sec. More gain would be desirable so that stabilization could be obtained with lower levels. This could be obtained by adding a second stage to the dc amplifier, a modification which is possible with the present power supplies.

C. The Absorption Cells

The cells have been built from standard S-band waveguide, 1 1/2" x 3" in cross-section. Both contain a centrally located Stark electrode made of 1/16" copper with some small holes drilled in them to assist pumping. The cell which was built first and has been used for HDO and CH_3I is 20' long. Mica windows are used at the ends. Since this cell employs polystyrene insulation and relies upon wax for vacuum seals, it may not be heated for outgassing.

The second cell, which has been used for CH_3Br, is 10' long, and was designed to be heated to 150°C for outgassing. The insulation is made of teflon, and gasket type seals were employed originally. The heat for outgassing is supplied by six 250 watt infra-red lamps. Unfortunately, the gaskets have not been reliable, and it has been necessary to resort to wax on some of the seals for routine operation.

Polyfoam insulation is available for both cells, and with it they may be cooled with dry ice. The pumping system employs an

Eimac HV-1 oil diffusion pump with a rated pumping speed of 67 liters/sec. Each cell is equipped with a 1946 thermocouple gauge, and sometimes these are supplemented by ionization gauges.

The rf input comes through flexible coaxial line to an adapter at one end of each cell. A waveguide type tunable crystal holder is used at the receiving end. 1" x 2" C-band components with tapered transition sections are available for connection to the sending and receiving ends of the cells. These are used as a high pass filter to separate effects due the fundamental of an S-band oscillator tube from those produced by its second harmonic in situations in which a doubt arises.

D. The Square Wave Generator

The circuit of square wave generator supplying the Stark voltage is shown in Figure 4, and its power supply is shown in Figure 5. This generator has been modified from a circuit due to Hillger.[5] The original circuit employed 3C45 hydrogen thyratrons in the final stage. We were unable to obtain reliable operation using these tubes. Therefore, the circuit was changed to use 811 high vacuum tubes. The waveform deteriorated somewhat as a result of the change, but the generator now is reasonably reliable.

A multi-vibrator supplies through amplifiers and blocking oscillators grid pulses alternately to the 811's. When the upper 811 receives a pulse the Stark electrode is connected through

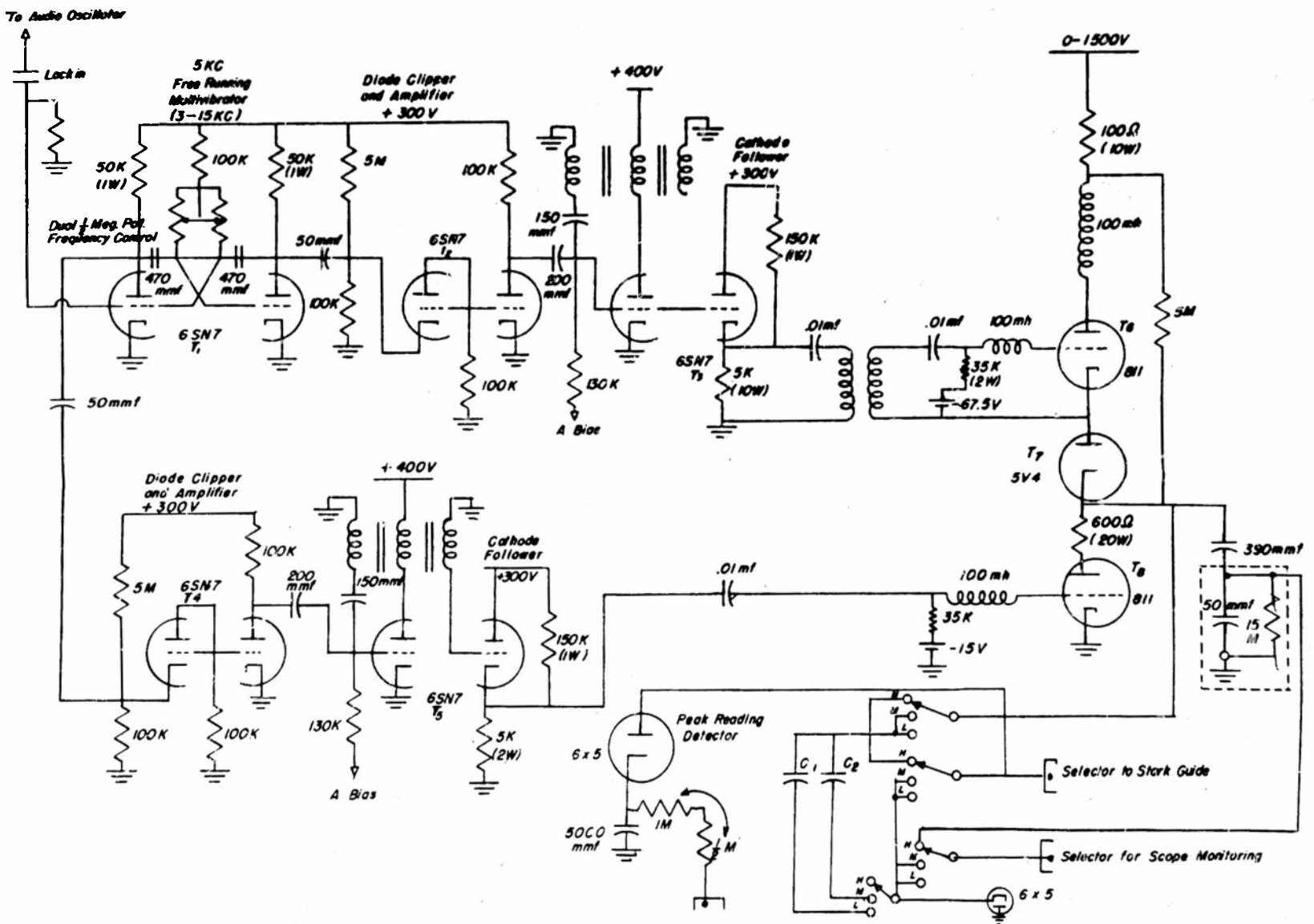

FIG. 4 Square Wave Generator

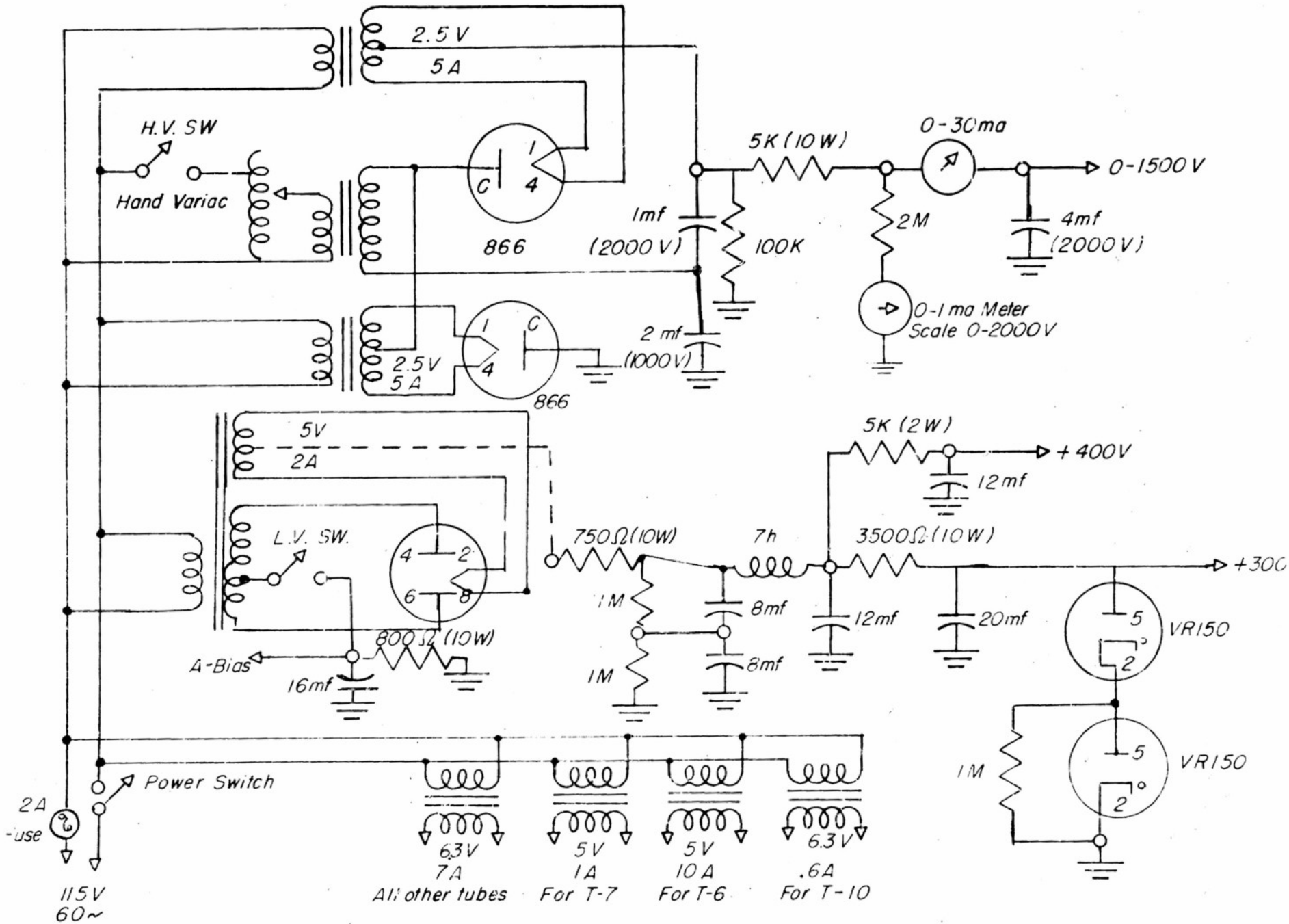

FIG. 5 Power Supply for Square Wave Generator

the tube to high voltage and becomes charged. When the lower 811 receives a pulse, the electrode is discharged through this tube to ground. A diode peak-reading voltmeter is also included in the instrument.

For frequency stabilization, the multivibrator is weakly coupled to an af signal generator of high stability. The output is monitored by observing the 1:1 Lissajous pattern on an oscillopscope whose horizontal voltage is derived from the stabilizing signal generator. The output voltage is continuously variable up to 1000 volts. The top of the square wave has a slope of about five percent near maximum voltage. The base of the square wave increases slowly up to about 25 volts as the top is increased to 500, and then the base rises rapidly to about 300 volts as the top approaches 1000.

E. The Amplifiers

The amplifiers and phase-sensitive detector are located in two units. The preamplifier, shown in Figure 6, employs three 6SJ7 tubes, the first two being pentode amplifiers, and the third being a triode cathode follower. The measured noise figure is about 4db. This noise figure could only be obtained by using a high-fidelity af transformer at the input. Also measurements indicated that care should be exercised in isolating the input transformer from strong ac magnetic fields. While the above noise figure could be improved by the use of a triode circuit, little advantage would

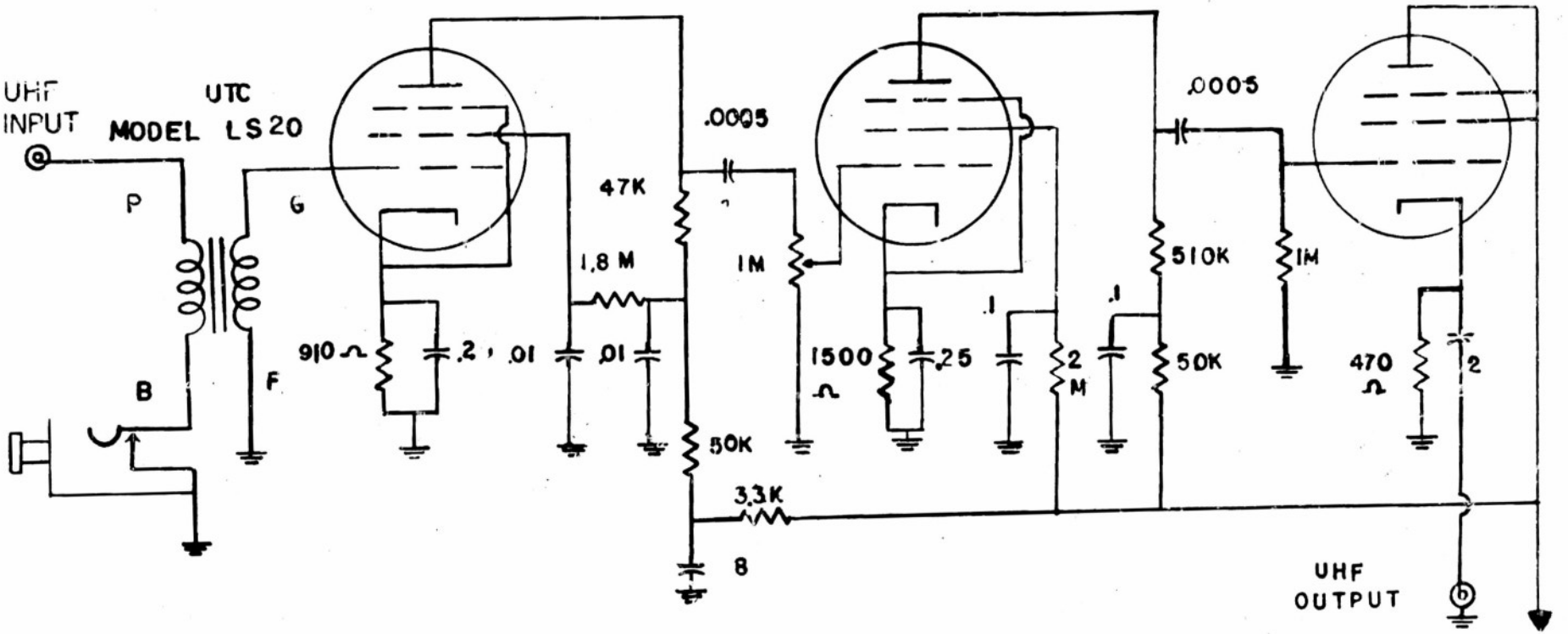

NOTE: ALL CONDENSERS IN MICROFARADS

FIG.6 PREAMPLIFIER

result since most of the noise in the system appears to originate in either the oscillator tube or the crystal detector.

The circuit of postamplifier and phase-sensitive detector, shown in Figure 7, is modified from one due to Beringer.[6] The first stage employs a 6SJ7 twin-"T" tuned amplifier. This is followed by a 6SL7 phase inverter which drives the control grids in push-pull of two 6SJ7 detector tubes. The reference voltage is applied to the suppressor grids of these tubes in parallel. Beringer's original circuit operated at 30 cps. Because of the increase of the frequency to 5000 cps it was possible to reduce many of the RC time constants in the stages ahead of the detector to improve discrimination against power supply ripple. On the other hand at this higher frequency extreme care in regard to length of leads and placement of parts had to be employed to prevent oscillation. Also the cathode circuit of the detector had to be redesigned to prevent a parasitic oscillation.

The present circuits have evolved from a series of modifications. With the present version, the stability is satisfactory, and the gain is more than adequate. Except with a very low rf input, the gain is so great that generally a 20 db attenuator is connected between the two units: otherwise the gain controls are near to their "off" positions and are hard to adjust.

F. The Frequency Standard

A block diagram of the frequency standard is shown in Figure 8. The heart of the instrument is the transmitter portion

FIG. 7 PHASE SENSITIVE DETECTOR

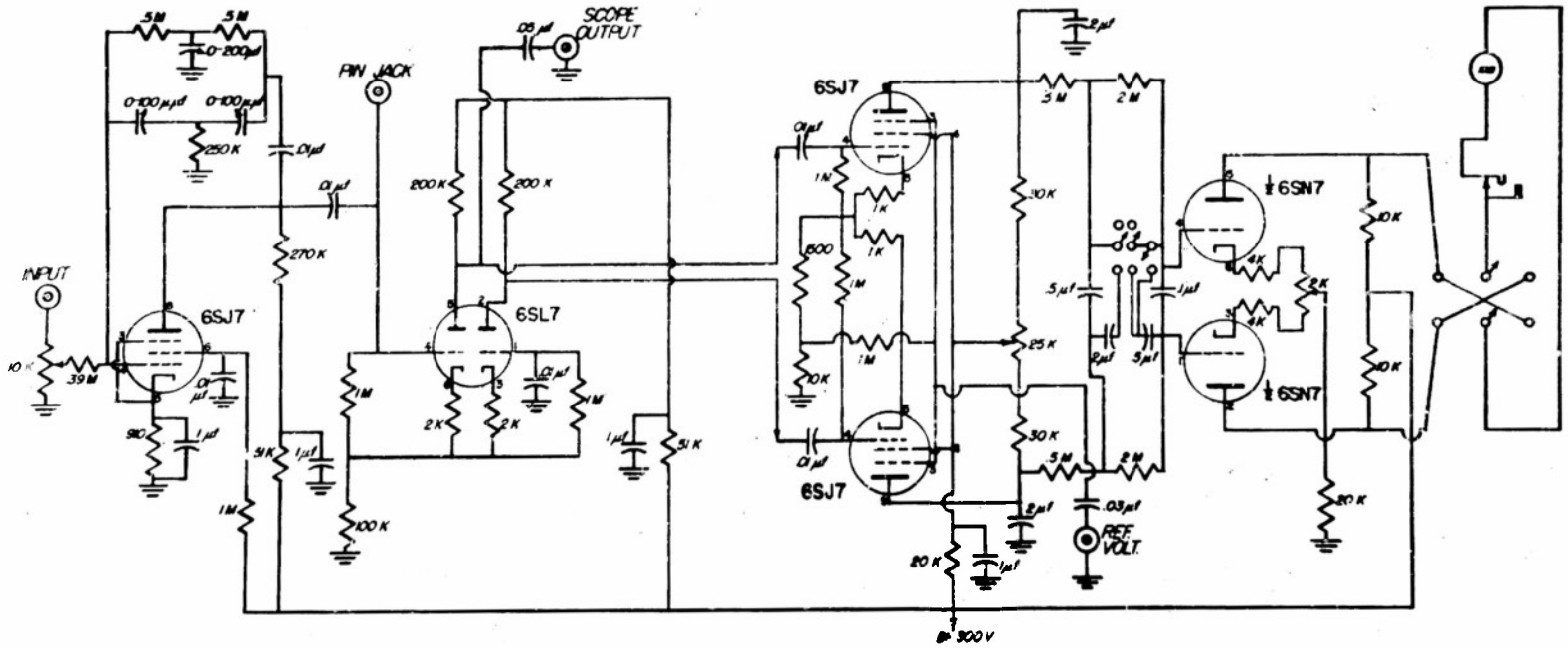

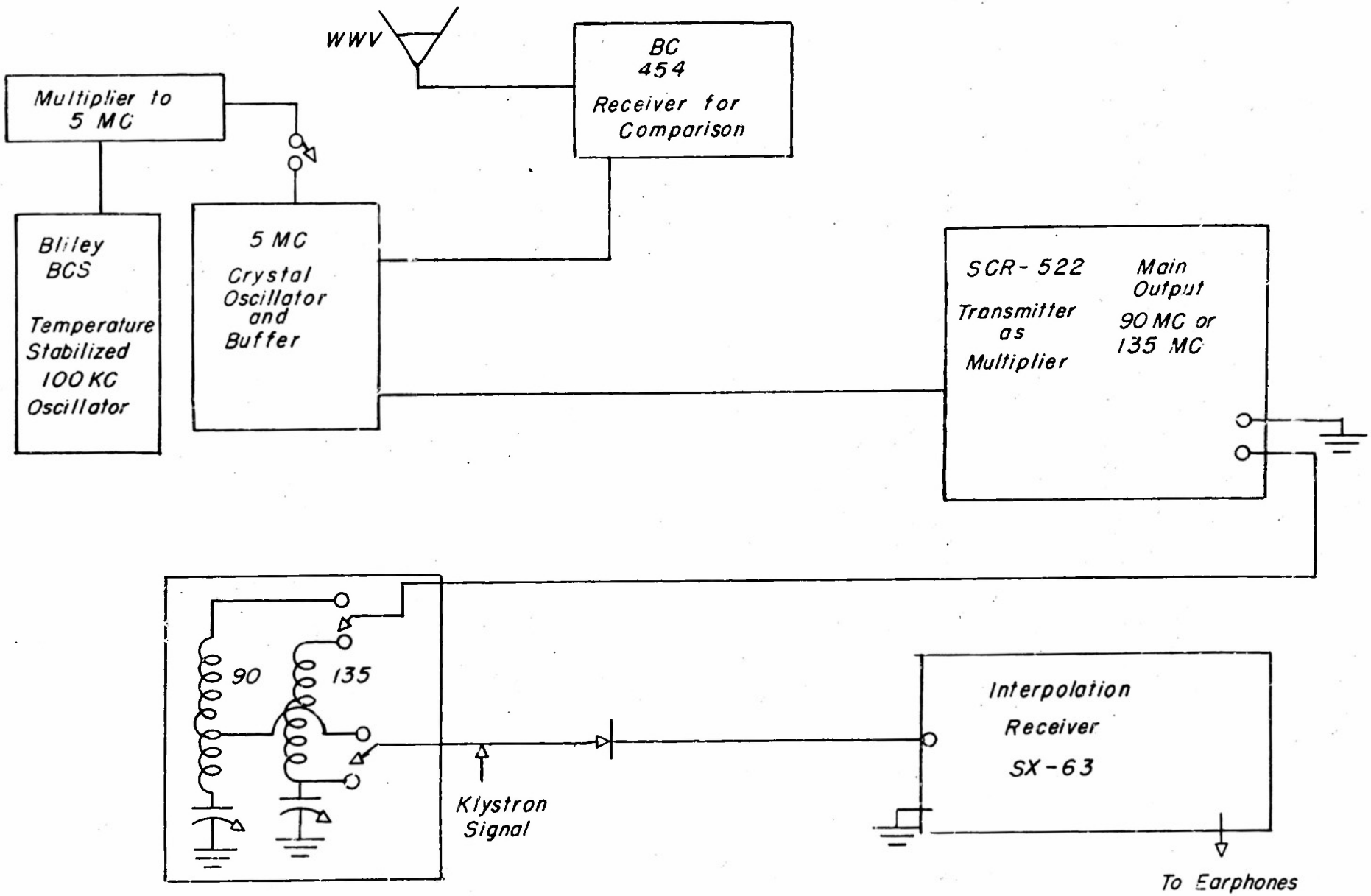

FIG. 8 Block diagram of frequency standard.

of a SCR-522 war surplus radio. The original output frequency was variable from 95 to 156 Mc/sec, but by padding the tuned circuits with small condensers, output is now obtained at 90 or 135 Mc/sec. This output is applied to a 1N21B silcon crystal which generates harmonics of sufficient strength in the S-band and uhf regions. The frequency of the klystron is compared to an appropriate harmonic by feeding the output of the multiplier chain and some power from the oscillator to another 1N21B crystal whose output feeds an SX-63 interpolation receiver. When the SX-63 receiver is employed in the stabilization circuit shown in Figure 2, a second interpolation receiver, a war surplus BC-639-A, may be employed to monitor the operation. To eliminate some spurious responses, it has been necessary to connect at the output of the SCR-522 transmitter a high-pass filter with a cut-off at about 40 Mc/sec (Eldico type TVR-62). This filter is not shown in Figure 8.

In routine search work, the input of the SCR-522 transmitter is derived from its own crystal oscillator using a selected but not stabilized 5 Mc/sec quartz crystal. With this the accuracy is about 0.5 Mc/sec at the S-band. When the system for stabilizing the frequency of the klystron is employed and when the desired frequency lies close to a harmonic of the frequency standard of half wave between, the system becomes inoperable because of the confusion arising from two responses. In this situation the 5 Mc/sec crystal is replaced by another of very different frequency.

For making final measurements of the frequency of a line, the input is derived indirectly from a Bliley BCS temperature stabilized 100 kc/sec oscillator. The rated stability is two parts in a million over a period of a month. The frequency of this may be synchronized with the 5 Mc/sec frequency of WWV by the use of a war surplus BC454 receiver which has been equipped with a magic eye tube connected to its second detector load resistance. The BCS oscillator is followed by a chain of multipliers delivering an output at 5 Mc/sec. The circuit of this chain of multipliers, which is of our own design and construction, is shown in Figure 9. When these units are employed, a switch on the SCR-522 transmitter is thrown to disconnect the grid of the first tube from the 5 Mc/sec crystal to the output of the multiplier chain, and another section of the same switch short-circuits the inductance in series with the cathode of this tube so that it is prevented from oscillating.

When the input is derived from the BCS unit, the principal response is usually accompanied at 100 kc/sec intervals by one or two satellites on either side. Since these are generally weaker, there is little difficulty in distinguishing them from the principal response, and sometimes these have been used to obtain more accurate interpolation. For some situations, it has been advantageous to produce more remote satellites with usable intensity. These may be produced by making an improvised connection between one of the output terminals of the BCS unit to the ungrounded terminal of the milliameter used to measure the current of the 1N21B harmonic generator.

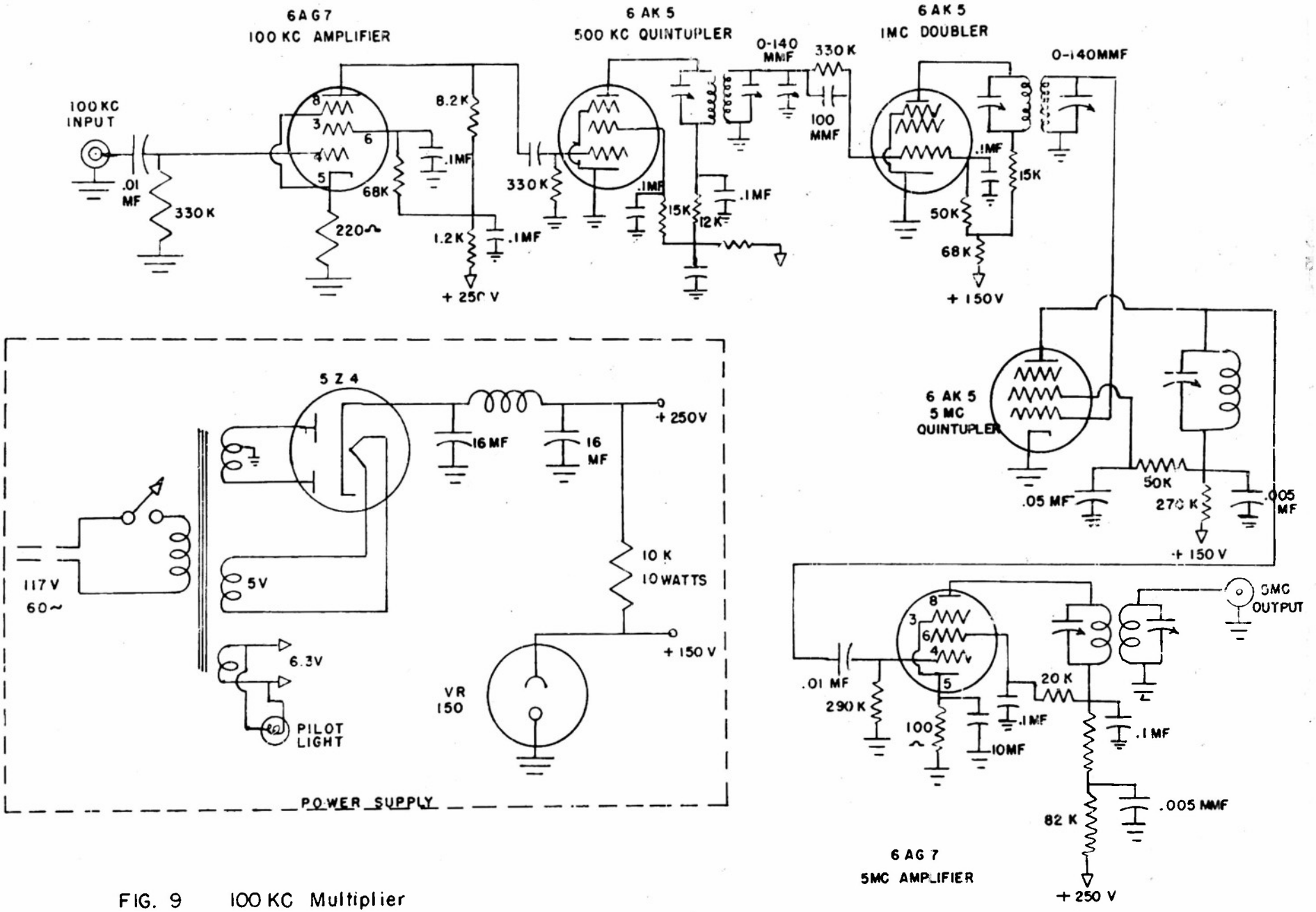

FIG. 9 100 KC Multiplier

G. Ultra-High-Frequency Operation

Present operation below 1000 Mc/sec employs the 1 1/2" x 3" x 20' absorption cell. Since the cut-off of its TE_{01} mode occurs at 2000 Mc/sec, this cell must be operated as a parallel plate transmission line in a TEM mode, the characteristic impedance being about 50 ohms. Both the rf input and the Stark voltage are applied through an L-C decoupling network to the Stark electrode at a terminal about 4" from the sending end. The location of this terminal was selected before the modification for uhf operation was contemplated. The actual end of the cell is closed either with its original mica window or by a metal plate. To obtain a good impedance match at the sending end it is necessary to use a variety of procedures depending upon the particular frequencies: variation of the cable lengths between the oscillator and the cell and between the cell and the frequency standard, the introduction of an S-band double stub tuner at some critical position in the oscillator line, or the connection of a variable condenser on this line with a "T" connector.

At the receiving end there was first used a special adapter which made capacitative coupling to the Stark electrode through the original mica window. This adapter was connected to a coaxial crystal mount through an impedance matching arrangement which consisted of an S-band double stud tuner assisted by some male-to-male and female-to-female coaxial adapters acting as line stretchers. This termination gave satisfactory performance in the region of 825 Mc/sec but was inadequate at 500 Mc/sec. Therefore it has been replaced by one employing

a new adapter which allows a direct connection to the Stark electrode. The impedance matching network consists of a double-tuned circuit employing lumped constant parameters. The primary is series-tuned to prevent short-circuiting the Stark voltage while the secondary is parallel-tuned to provide a dc return for the crystal detector.

The source of rf employed in this region is the 6AF4 triode local oscillator tube of a Mallory TV-101 uhf television converter. Output is derived by introducing a small coupling loop into the shielding compartment containing the bottom of the tube socket. The frequency is variable between about 400 and 850 Mc/sec. The frequency stability is very good. Even at the high end of the range and even without stabilizing the supply voltages, the frequency generally remains within audio beat range of a reference frequency for minutes at a time. However, generally the input is stabilized by the use of a saturated iron regulator, and sometimes the plate voltage is obtained from "B" batteries.

A crude Lecher wire has been found to give preliminary values of frequency with an accuracy of a percent or two, quite adequate for distinguishing between responses of the frequency standard below 850 Mc/sec.

In an attempt to improve the signal-to-noise ratio at 825 Mc/sec an experiment was made with superheterodyne detection. A second Mallery TV-101 converter was obtained, and a 1N34 second detector

was installed at the output of its 90 Mc/sec IF amplifier. The $3_2 \rightarrow 3_3$ line of HDO was observed both with this superheterodyne detector and with the original crystal detector at a low rf power level, corresponding to a rectified current of 5 microamperes. The signal-to-noise ratio with the superheterodyne detector was at best barely equal to that with the crystal detector. Furthermore it was observed that as the frequency of the oscillator was greatly detuned, the noise output of the amplifier decreased considerably. Therefore it appears, at least at this frequency, that the oscillator rather than the detector is the principal source of noise in the system.

Because of the narrow bandwidth of the rf system, it has been necessary to employ an unconventional procedure for searching for lines. First, the system is tuned up at a suitable frequency near to where the line is to be expected, and then, with the frequency fixed, the Stark voltage is swept, causing the Stark components to be brought one by one on to the frequency of operation. Then the process is repeated at several other frequencies nearby. From the data consisting of the frequencies and the corresponding voltages an approximate value of the frequency of the unsplit line is found by extrapolation. Then for final measurements the system is tuned up on this extrapolated frequency, and, with the Stark voltage constant, the frequency is swept by applying motor drive to the tuning control of the oscillator. The interval which can be covered reliably by this method is quite small, usually hardly more than 1 Mc/sec. Therefore,

it is generally necessary to retune at several adjacent frequencies and repeat the observations before the line is found.

The preliminary search made with fixed frequency and variable voltage is hampered by errors in the voltage measurement and by variations of direct pick-up voltage which make the base line on the record non-uniform. To reduce these difficulties, it is planned for future work of this type to use a variable dc power supply as the principal source of Stark voltage. Superimposed upon this dc voltage will be a small square or sine wave for modulation purposes.

H. Sensitivity

The calculated minimum detectable absorption coefficient is roughly 10^{-10} cm^{-1} in the S-band region. This value is consistent with the calculated intensity and observed signal-to-noise ratio of S-band HDO lines.

The calculated value is based upon the values of 20' for the length of the absorption cell, 20 cps for the noise bandwidth, and 100 microwatts for the rf power. If a value of 60 for the figure of merit of a square law crystal is employed in the formula due to Gordy,[7] the calculated value of the minimum detectable absorption coefficient is 1×10^{-10} cm^{-1}. Using a value for the noise figure of 3 in the formula due to Townes and Geschwind,[8] a value of 2×10^{-10} cm^{-1} is obtained. Although based upon slightly different assumptions and different data concerning the detector, these values are in [illegible]-

reasonable agreement. A power level of more than 1000 microwatts, instead of 100, is often obtainable and, at a high gas pressure, it can usually be used without saturating the sample, and thus somewhat greater sensitivity is often obtainable. Also in the uhf region figures of merit of crystals should be better, and thus still better sensitivity should be obtainable there.

III INVESTIGATIONS OF SPECIFIC MOLECULES

A. HDO

1. Introduction

The first molecule to be investigated was half-heavy water (HDO) because of several reasons. This molecule is of considerable interest from the theoretical point of view since with it centrifugal distortion effects are large, and thus the study of it leads to the opportunity to check the validity of theories of centrifugal distortion. In addition, knowledge of the location of lines and their absorption coefficients is of considerable interest to meteorologists and to those concerned with calculating the absorption of radio waves in the atmosphere with the object of finding suitable frequency bands for radar and radio. At the time this investigation was started only four HDO lines had been found previously by microwave methods, [9, 10] and this number was completely inadequate for evaluating the constants of the molecule. At the same time the published calculations of King, Hainer and Cross[11] clearly indicated the possibility of observing several lines in the frequency region below 3000 Mc/sec.

It should be pointed out that the HDO species of water has a spectrum which qualitatively differs from the spectra of the single isotope species, H_2O and D_2O. Because with HDO the dipole moment is oblique to both the axes of least "a" and intermediate "b" moment of inertia instead of coinciding with the "b" axis, the selection rules

are considerably less restrictive. These rules permit the observation of Q-branch ($\Delta J = 0$) lines as well as the P- and R- branch ($\Delta J = \pm 1$) lines which are observable with H_2O and D_2O. Thus there is considerably greater possibility with HDO of observing in the microwave region an adequate number of lines. In fact all but one of the lines discovered by this project are of the Q-branch type. At the same time, data obtained with HDO may be employed to evaluate the structure of H_2O and D_2O.

2. Observations

The lines which have been discovered by this project are given in Table 1 along with their calculated absorption coefficients. These coefficients were modified from those obtained by King, Hainer, and Cross[11] by the use of the line width parameter 0.38 cm^{-1} due to Strandberg[10] and in some case by the use of revised values of the

Table I

Measured Lines of HDO

Transition ($J_\tau \rightarrow J_\tau'$)	Measured Frequency (Mc/sec)	Absorption Coefficient (cm^{-1})
$5_2 \rightarrow 5_3$	486.50 ± 0.15	1.5×10^{-8}
$3_2 \rightarrow 3_3$	824.64 ± 0.05	1.5×10^{-7}
$6_1 \rightarrow 6_2$	2394.56 ± 0.05	2.9×10^{-7}
$4_0 \rightarrow 5_{-5}$	2887.4 ± 0.1	1.5×10^{-8}
$12_{-1} \rightarrow 12_0$	2961 ± 1	1.6×10^{-9}
$9_0 \rightarrow 9_1$	3044.71 ± 0.10	3.4×10^{-8}

frequency. The observed intensities were roughly consistent with the calculated ones. Some of these data have been published in preliminary form[12,13,14].

Four of the lines could be positively identified by their well resolved Stark patterns. Two of these are shown in the illustrations of a previous preliminary report of this work[14]. Stark information gave circumstantial evidence for the identification of a fifth line, the $4_0 \rightarrow 5_{-5}$, since the calculated coefficient for it was very small, and no resolved splitting was observed with this line. This tentative identification was confirmed by Benedict[15] on the basis of his work in the infrared. The identification of the $12_{-1} \rightarrow 12_0$ line is not completely definite since a line of comparable intensity was observed at 2991 Mc/sec, and neither it nor the one at 2961 Mc/sec had splittings which could be resolved. However, because of the almost perfect agreement of 2961 Mc/sec with the calculated value of the frequency of the $12_{-1} \rightarrow 12_0$ line, it appears that the present assignment is correct. Apparently the line at 2991 Mc/sec is due to some contaminating vapor.

As of October 31, 1953, three Stark components of the $5_2 \rightarrow 5_3$ line had been observed at two or three frequencies by the fixed frequency-variable voltage search method. The unsplit line was not found and measured until somewhat later, while this report was in preparation.

3. Analysis of Data

We have made a detailed analysis of Q-branch, transitions for which $\Delta J = 0$ and $\Delta K_{-1} = 0$. The principal parameters involved are

$$\frac{a - c}{2} \quad \text{and} \quad \kappa = \frac{2b - a - c}{a - c},$$

where a, b, and c are the rotational constants respectively relative to the principal axes of least, intermediate, and greatest moments of inertia. The rigid rotor frequencies have been calculated by the methods of King, Hainer, and Cross[16]. However, with such a light molecule, centrifugal distortion effects are large, and the rigid rotor approximation is very inadequate. Recently Kivelson and Wilson[17], using first order perturbation theory, have derived a formula for correction of rigid rotor frequencies which may be applied to Q-branch transitions. For purposes of analysis, it is convenient to write this formula as follows:

$$f = f_o \left\{ 1 + J(J+1)(Kx + y) + K(K^2 + 2)B + K(K-1)(2K-1)C + K(K^2-1)D \right\} . \qquad (1)$$

where K is the K_{-1} index of the two levels which combine to give the transition, and J is the quantum number of total angular momentum. f_o is the rigid rotor frequency, and f is the corrected frequency. The quantities x, y, B, C, and D are closely related to the centrifugal distortion parameters δ_J, D_{JK}, R_5, D_K, and R_6. Since f_o depends depends upon κ and $(a - c)/2$, there are seven adjustable parameters. These are selected to obtain the best possible fit with observed frequencies. In our work, constants were adjusted to fit

nine lines. Since this calculation was performed, four additional lines have been found. These results are shown in Table II. The four lines denoted by asterisks in the first column are the ones which were not employed in the evaluation of the constants. It may be seen that the agreement is very good except in the case of the

Table II

Q-Branch Transitions of HDO

Transition ($J_\tau \rightarrow J_{\tau'}$)	Distortion Correction (Mc/sec)	Measured Frequency (Mc/sec)	Measured -Calculated Frequency	Reference
$2_1 \rightarrow 2_2$	-79.44	10,278.99	-0.01	10
$3_0 \rightarrow 3_1$	-469.87	50,236.90	+0.02	10
$3_2 \rightarrow 3_3$*	-14.95	824.64	+0.03	This work
$4_1 \rightarrow 4_2$	-118.87	5,702.78	+0.01	18
$5_0 \rightarrow 5_1$	-540.98	22,307.67 22,309.	-0.02	10 9
$5_2 \rightarrow 5_3$*	-17.52	486.50	+0.03	This work
$6_1 \rightarrow 6_2$	-98.20	2,394.56	+0.07	This work
$7_0 \rightarrow 7_1$	-402.24	8,577.7	-0.20	18
$8_{-1} \rightarrow 8_0$	-1336.12	24,884.77 24,884.85	+1.53	18 19
$9_0 \rightarrow 9_1$	-238.78	3,044.71	+1.24	This work
$10_{-1} \rightarrow 10_0$*	-785.13	8,836.95	+6.42	18
$11_{-2} \rightarrow 11_{-1}$*	-2269.64	22,581.1	+30.2	18
$12_{-1} \rightarrow 12_0$	-403.82	2,961.	-2	This work

$11_{-2} \rightarrow 11_{-1}$ line, which, however, has a very large distortion correction. The values of the constants which were employed are shown in Table III.

Table III

Constants Evaluated from Q-Branch Transitions

Constant	Value
κ	-0.6830
$\frac{a-c}{2}$	2.54495×10^{5} Mc/sec
x	-0.59612×10^{-4}
y	-1.47052×10^{-4}
B	-3.3569×10^{-4}
C	8.9140×10^{-4}
D	-12.3185×10^{-4}

From the analysis of P- and R-branch transitions, two additional constants are evaluated. These are another distortion constant D_J and $(a + c)/2$, where a and c have their previous definition. For this purpose it is convenient to write the total rotational energy as follows:

$$W = \frac{a + c}{2} J(J + 1) - D_J J^2 (J + 1)^2 + E, \qquad (2)$$

where E is the so-called "reduced energy". E is evaluated from the reduced energy matrices (including centrifugal distortion)[20]. The elements of these matrices are evaluated in terms of the constants determined from the analysis of Q-Branch transitions.

Using the values $(a + c)/2 = 4.456524 \times 10^5$ Mc/sec and $D_J = 6.71064$ Mc/sec a "best fit" was obtained with the three observed transitions of this type. Data on these transitions are shown in Table IV.

Table IV

P- and R-Branch Transitions

Transition ($J_\ell \rightarrow J_{\ell'}$)	Measured Frequency (Mc/sec)	Measured - Calculated Frequency	Reference
$4_{-3} \rightarrow 3_1$	20,460.4	-184.8	10
$4_0 \rightarrow 5_{-5}$	2,887.4	-230.7	This work
$6_{-2} \rightarrow 7_{-6}$	26,880.38 26,880.47	+323.4	18 19

Since there was some doubt as to whether the 4_0 is higher or lower than the 5_{-5} and whether the 6_{-2} level is lower or higher than the 7_{-6} level, calculations were made with all four of the possible combinations. Meaningless results were obtained except with the assignment indicated in Table IV: that is, with the 4_0 and 6_{-2} being the lower levels.

With reference to the paper of Kivelson and Wilson[17] distortion constants in conventional form may be computed from the constants given in Table III. Posener and Strandberg[18] have calculated values of the same constants from essentially the same data but using reduced energy matrices in the analysis of Q-branch transitions as well as with P- and R-branch ones. They have also computed "theoretical" values of these constants from infrared data. All of these results are shown in Table V.

Table V

Parameters of HDO

Parameter	Posener and Strandberg[18]		This Work
	Theoretical	Observed	Observed
$(a + c)/2$	4.4487×10^5 Mc/sec	$4.484 \pm .002 \times 10^5$ Mc/sec	$4.457 \pm .006 \times 10^5$ Mc/sec
$(a - c)/2$	2.5301×10^5 Mc/sec	$2.555 \pm 0.005 \times 10^5$ Mc/sec	$2.545 \pm .001 \times 10^5$ Mc/sec
κ	-0.68120	-0.6841 ± 0.0002	$-0.6830 \pm .0003$
D_J	9.2418 Mc/sec	11.6 ± 2.0 Mc/sec	6.7 ± 2.5 Mc/sec
D_{JK}	36.8132 Mc/sec	36.8 ± 0.5 Mc/sec	68.9 ± 0.5 Mc/sec
D_K	287.0893 Mc/sec	287 ± 5 Mc/sec	627 ± 10 Mc/sec
δ_J	3.3331 Mc/sec	3.333 ± 0.005 Mc/sec	$4.168 \pm .010$ Mc/sec
R_5	-7.8772 Mc/sec	-7.877 ± 0.010 Mc/sec	$-10.156 \pm .010$ Mc/sec
R_6	-0.5722 Mc/sec	-0.572 ± 0.005 Mc/sec	$-1.604 \pm .010$ Mc/sec
$R_7^{(x)}$	3.1160 Mc/sec	3.12 ± 0.05 Mc/sec	----------
$R_8^{(y)}$	-8.1994 Mc/sec	-8.20 ± 0.05 Mc/sec	----------
$R_9^{(y)}$	49.9173 Mc/sec	50.0 ± 0.5 Mc/sec	----------

Posener and Strandberg have contended that the Kivelson-Wilson formula, Eq. (1), is an approximation and, therefore, even if it can be made to fit the data very well, it should be regarded as a semi-empirical formula. Accordingly, the distortion constants derived from it are of questionable physical significance and cannot be expected a priori to correspond to the actual constants of the molecule. These contentions are supported by the results of Table V, where it may be seen that our values of the distortion constants are generally in poor agreement with the theoretical ones while theirs are in good agreement.

Further evidence may be inferred from the fact their calculated frequencies of the P-and R-branch transitions agree with the observed ones much better than ours.

Other aspects of these results, however, suggest that the Kivelson-Wilson formula is useful for some applications. When it can be used, it is a great convenience as the labor required for any degree of accuracy is considerably less than that required with the reduced energy matrices. It is to be noted that although our distortion constants are in poor agreement with the theoretical values, our rotational constants, $(a - c)/2$, $(a - c)/2$, and K, are in good agreement, in fact, in slightly better agreement than theirs. This observation suggests that our procedure of using the formula for analysis of the Q-branch transitions and using the reduced energy matrices only with the P- and R-branch transitions (much fewer in number) may yield reliable values of the rotational constants with a saving of effort.

At the same time it should be noted that our fit to the Q-branch transitions is somewhat better than theirs. Their average deviation is about one part 1850 while on the same eleven lines ours is about one part in 3500. Neither set of calculated values fits the $11_{-2} \rightarrow 11_{-1}$ line very well, and if this is excluded, the comparison is even more favorable. The fact that our fit is somewhat better is probably to be attributed to the fact that because our method involves less labor it may be carried to a higher degree of numerical accuracy within a finite time.

The ability of the Kivelson-Wilson formula to fit observed data has withstood a severe test in this experiment. In spite of the fact that centrifugal distortion effects are large with HDO, the formula has been found with seven constants to give reasonably good fit with thirteen lines. These lines have ranged in J from 2 to 12 and in frequency roughly from 500 to 50,000 Mc/sec.

In Table VI are shown the values of the principal moments of inertia computed from our values of the rotational constants. Also given is the quantity $\Delta = I_a + I_b - I_c$. Classically for a rigid rotor Δ would be equal to zero. Its finite value is to be attributed to zero point vibrations. Also included are the values computed by Benedict, Gailar, and Plyler[21] from their infrared data. The agreement can be seen to be very good.

Table VI

Principal Moments of Inertia of HDO

(Units are gm $cm^2 \times 10^{-40}$)

Quantity	This Work	Benedict et al[21].
I_a	1.1982	1.196
I_b	3.0862	3.076
I_c	4.3887	4.360
Δ	0.1043	0.088

4. Study of the $3_2 \rightarrow 3_3$ Line of HDO for Hyperfine Structure

a) Introduction

Molecular rotational levels frequently have hyperfine splittings which are due to the interaction of nuclear quadrupole moments with the gradient of the electric field of the molecule. Hyperfine splittings due to the deuteron are of particular interest. The measurement of the splitting determines the product of the quadrupole moment and the gradient of the electric field. Since the deuteron is one of the few nuclei whose quadrupole moment is known, such a measurement with it gives the gradient of the field separately, and this is of considerable interest in the study of chemical bonds. Furthermore, since the deuteron has the smallest known non-zero quadrupole moment, these splittings are very small and their resolution offers a challenge to the experimenter.

The study of the $3_2 \rightarrow 3_3$ line of HDO offers a favorable opportunity for observing such a splitting. Because of the relatively low value of J, the splitting is relatively large as compared to other lines accessible with the present equipment. At the same time the intensity is large while the frequency falls in the uhf range where absolute frequency stability is easy to obtain. For these reasons, this line has been studied with the purpose of detecting a quadrupole effect. While no hyperfine splittings have been resolved, the shape of the line under experimental conditions yielding high resolution seems interpretable only in terms of quadrupole effects. In fact, it is possible to make some estimate of the magnitude of

the splitting. The observations will not be discussed, however, until it is shown what may be expected from theory.

b) Theory

Each of the original levels is split into three hyperfine levels as a result of the coupling of the nuclear spin $I = 1$ with the rotational angular momentum $J = 3$ to give values of the total angular momentum $F = 2$, 3, and 4 respectively. Such an energy level diagram and the transitions resulting from the selection rule $\Delta F = 0, \pm 1$ are shown in Fig. 10. Later it will be seen that there is reason to believe that the spacings of the two sets of levels are respectively nearly equal. Therefore the three $\Delta F = 0$ transitions occur at essentially the same frequency, and the remaining lines are located symmetrically with respect to this frequency. There is no expectation of determining the sign of the coupling constant because this determination requires a pattern of detectable asymmetry.

The intensities of these transitions are shown in Fig. 11. These have been calculated by standard methods[22]. The four satellite lines are theoretically only about three percent of the central line consisting of three $\Delta F = 0$ transitions. However, under experimental conditions their relative intensities are exaggerated. With the low gas pressure required for high resolution a condition of partial power saturation is inevitable, and since the satellites have smaller transition matrix elements, their intensities are not diminished as much by the partial power saturation. A similar effect in the microwave spectrum of ammonia is well known[23].

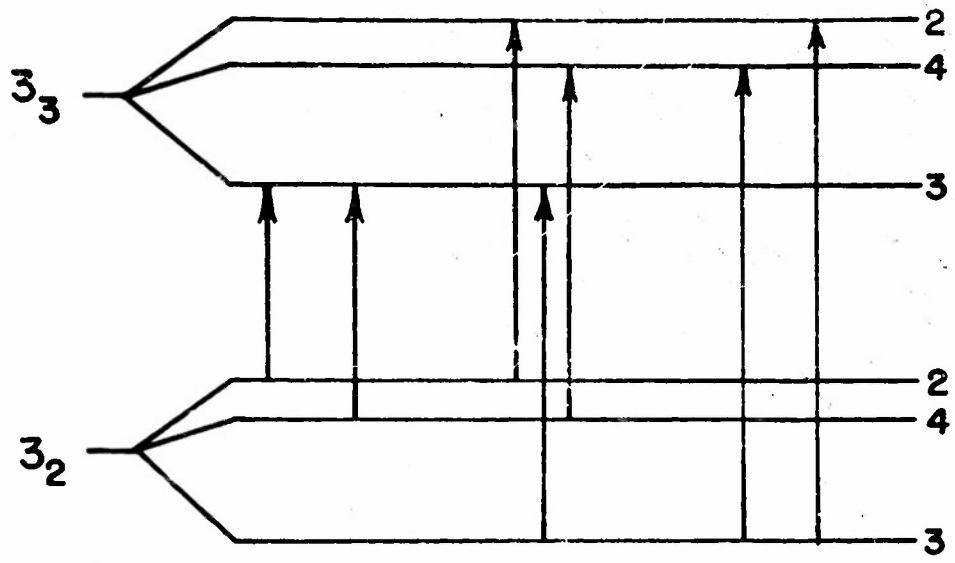

Hyperfine Levels of 3_2 and 3_3 States

FIG. 10

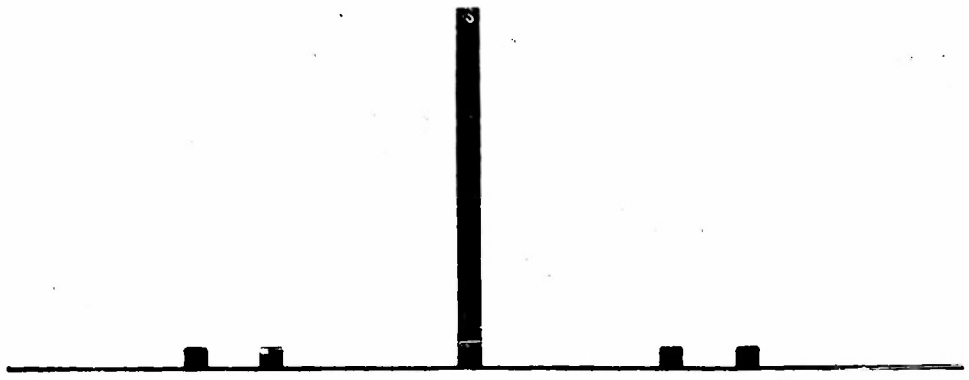

Hyperfine Splitting of 3_2-3_3 Line

FIG. 11

The magnitude of the spacings may be calculated by the theory due to Bragg[24] in terms of the Q-branch line strengths as evaluated by King, Hainer, and Cross[25]. Respectively for the 3_3 and the 3_2 levels the hyperfine splittings are given by the following resulting expressions:

$$W_3 = eQ\,(1.4936\ q_a + 0.2960\ q_b + 0.2104\ q_c)Y, \qquad (3)$$

and

$$W_2 = eQ\,(1.4958\ q_a + 0.2832\ q_b + 0.2210\ q_c)Y, \qquad (4)$$

where Q = quadrupole moment of the deuteron. q_a, q_b, and q_c are respectively the second derivatives of the electrostatic potential with respect to coordinates along the principal axes of least, intermediate, and greatest moments of inertia, and Y is Casimir's function.

$$Y = \frac{3/4C(C+1) - I(I+1)J(J+1)}{2I(2I-1)(2J-1)(2J+3)}, \qquad (5)$$

and

$$C = F(F+1) - I(I+1) - J(J+1).$$

For J = 3 and I = 1, Y has the values of 0.200, -0.250, and 0.083 for F = 2,3, and 4 respectively.

The above calculation is based upon first order theory only since this appears to have more than adequate accuracy for the present purposes. Furthermore, the 3_2 and 3_3 levels appear by inspection to be far removed from all J = 1,2, 4 and 5 levels, and therefore, the second order corrections probably are very small.

Only two of the quantities q_a, q_b, and q_c are independent. Since the potential satisfies Laplace's equation, $q_a + q_b + q_c = 0$.

Two important conclusions may be made from Eqs. (3) and (4). First, since the coefficients in these two equations are so nearly equal respectively, the hyperfine splittings of the 3_2 and 3_3 levels are probably very nearly equal. Secondly, from these equations it is possible to derive an approximate expression for the average separation of the four satellite lines from the central line in terms of the second derivative of the potential with respect to a coordinate along the O-D bond. To obtain another relation between the q's it is assumed that the field has azimuthal symmetry about the bond. Although the validity of this assumption is somewhat dubious from many points of view, the result of the present calculation can be considered a reliable approximation because of a very fortunate chance combination of the numerical values of the parameters. The bond is nearly parallel to the "a"-axis, the angle of inclination being about 17 degrees, and thus q_a is approximately equal to q, the second derivative of the potential along the bond. Any deviation from axial symmetry then affects mainly the values of q_b and q_c. On the other hand, it may be seen that in Eqs. (3) and (4) that the coefficients of q_a are very much larger than the others, and therefore the results are not seriously affected by errors in q_b and q_c.

This assumption implies a second relation between q_a, q_b, and q_c so that in principle now only one of these quantities is

independent, or q may be considered as being independent and q_a, q_b, and q_c may be expresed in terms of it by means of a tensor transformation. This transformation consists of multiplying q by Legendrian polynomials of order 2 whose arguments are respectively the cosines of the angles between the bond and the principal axes of inertia. When this calculation is performed and when the Bohr frequency postulate is applied, the result is

$$\Delta f = 0.426\ eQq, \qquad (6)$$

where Δf is the average magnitude of the separation of the four satellites from the central line and where eQq is expressed in terms of the same units as Δf.

c) Observations

In a preliminary report[13] we mentioned the observation of satellite lines 30 kc/sec on either side of the central line. As a result of helpful discussions with Mr. R. L. White and Professor C. H. Townes of Columbia University we have conducted further experiments which have shown that the effect was spurious, undoubtedly due to irregularities in the sweep of frequency. At the same time these experiments have uncovered an effect which appears genuine. The latter effect is a systemmatic change in line shape such that as the pressure is reduced the central portion of the line decreases in width more rapidly than the wings of the line. This behavior is consistent with the presence of the satellites which are expected from theory.

In Figure 12 is shown a recording of the line taken under conditions of high sensitivity and poor resolution. This illustrates the high intensity of this line. Barely visible on the baseline, which extends across the center of the record, are fluctuations due to noise. The upward off-scale deflection is due to the unsplit line, while the downward one is due to Stark components, which in this recording are not resolved. In Fig. 13 is shown another recording taken at greatly reduced pressure and with reduced power level. The line width has decreased at the expense of poorer signal-to-noise ratio. This recording is one of many which illustrate the abnormally intense wings of the line.

To put these observations on a subjective basis, the half-power, one-fifth power, and one-tenth power line widths were measured on a large number of recordings. The various ratios of these quantities were then plotted on graphs against the half-power line width. Ideally the pressure would be a more logical independent variable, but it was not convenient to measure the pressure since the range which was of interest lay in the transition region between thermocouple gauge and ionization gauge measurements. Therefore, the half-power line width, which can be assumed to vary continuously with pressure, was used as an independent variable. The plot of the ratio of one-tenth power to one-half power line width is shown in Fig. 14. At high pressure the ratio is near to the value 3 expected from the Lorentz theory of line shapes. As the pressure is decreased the ratio systematically rises. This effect

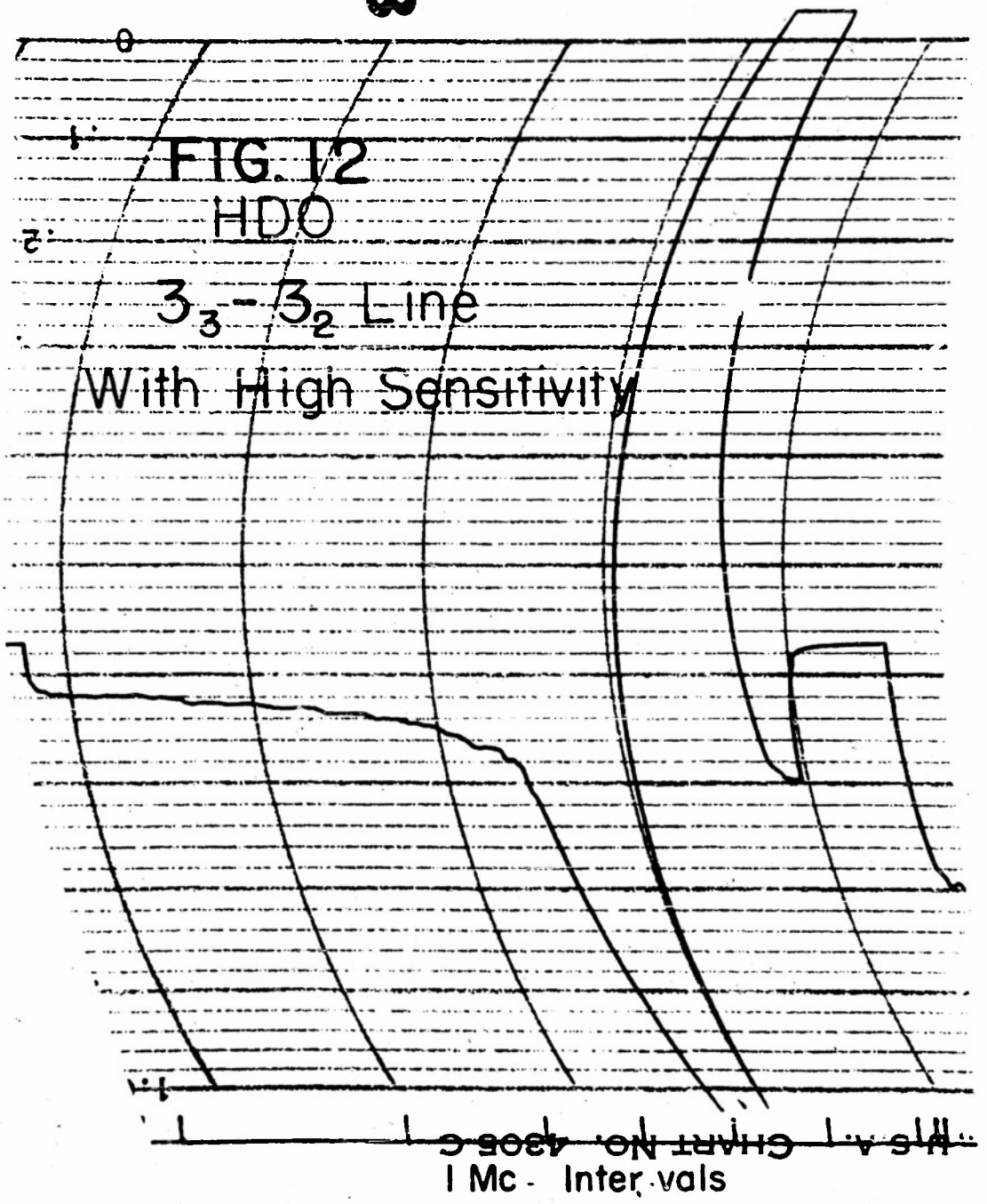

FIG. 12
HDO
$3_3 - 3_2$ Line
With High Sensitivity

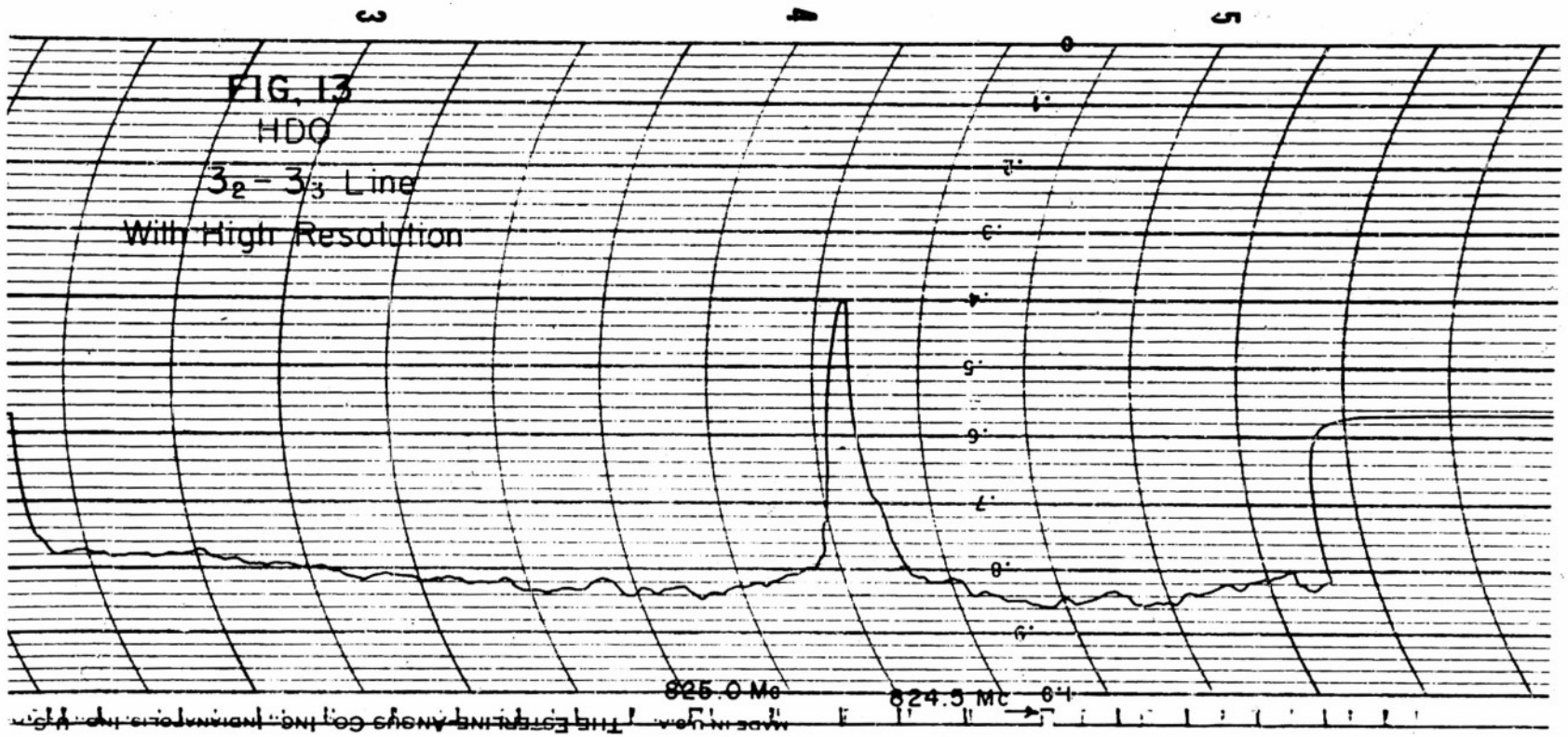

FIG. 13
HDO
$3_2 - 3_3$ Line
With High Resolution

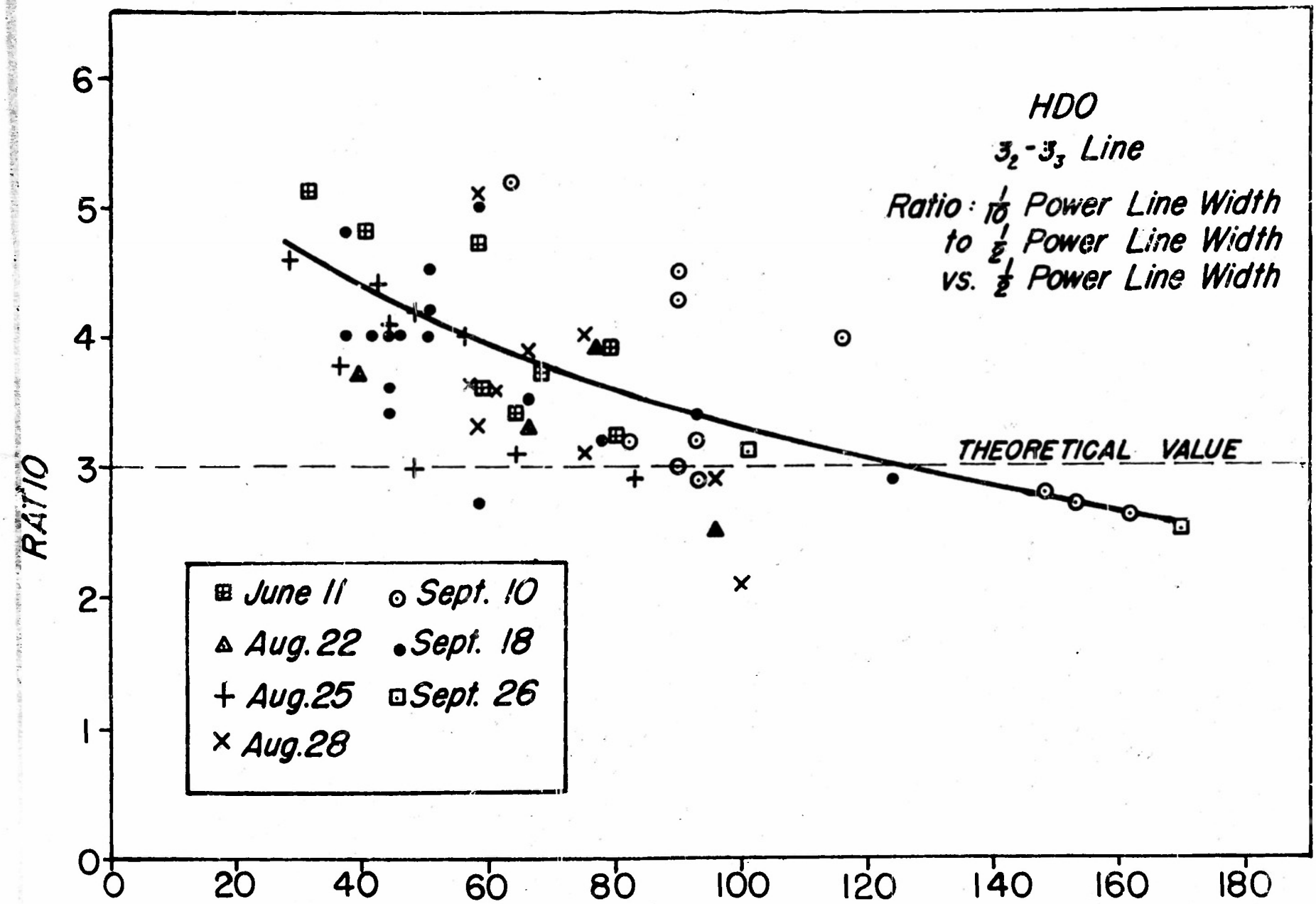

FIG. 14 HALF POWER LINE WIDTH (KC/SEC)

is definit in spite of the large scatter of the points which is due to many causes: irregularities in the sweep of frequency, irregularities in chart speed, experimental errors in the measurement of the record, and variation of conditions such as power level and rf tuning. In the observations of September 18, for only one of twelve successive recordings did the ratio fall below the theoretical value of 3. (The recording shown in Fig. 13 is one of this set. Its ratio was measured as 4.5 and its half power line width as 50 kc/sec).

A smooth curve drawn through the points on a similar plot of the ratio of one-tenth power line width to one-fifth power line width versus one-half power line width is at high pressures horizontal near the theoretical value of 1.5 and at low pressures bends upward reaching a value of about 2.0. On the other hand, a similar plot of the ratio of one-fifth power line width to one-half power line width shows no trend whatsoever away from the theoretical value of 2.0.

For interpretation of these, a series of theoretical line shapes based upon the spectrum shown in Fig. 11 were plotted for various values of the half-power line width relative to the average satellite spacing Δf. As the line width decreases the ratio of one-tenth power line width to one half power line width reaches a maximum value of 4.1 and then decreases, and the ratio of one-tenth power line width to one-fifth power line width goes through a maximum value of 2.0. The fact that the experimental values of these

ratios often exceed these maximum theoretical values may be attributed to the power saturation effect mentioned early. On the other hand, the presence of satellites has little effect on the one-fifth power line width, and the theoretical curves show, along with the experimental data, no significant variation in the ratio of one-fifth power line width to one-half power line width.

One estimate of the magnitude of the satellite spacing Δf may be obtained by noting that the maximum value 4.1 of the ratio of one-tenth power to one-half power line width occurs according to the theoretical curves approximately when the total half power line width is $0.46\,\Delta f$. By noting then where the smooth curve goes through the value of 4.1 in Fig. 14, the value of 93 kc/sec is obtained for Δf. This result is subject to the indeterminant error resulting from the distortion of line shape due power saturation. Another value was obtained by measuring the centers of the wings of the line in a number of recordings of the line made at high resolution. A value of 141 kc/sec was obtained. If the average value 117 kc/sec is substituted into Eq. (6), the value 272 ± 90 kc/sec is obtained for eQq. This value is in reasonable agreement with those obtained by White[26], who has measured values of $+175 \pm 20$ kc/sec for DCCCl and 300 ± 150 kc/sec for DCN.

The description of these observations would be incomplete without a discussion of some of the experimental conditions. The minimum recorded half-power line width was about twice the value of 15 kc/sec computed[27] for collisions with the walls and Doppler

broadening. There were several instrumental effects which contributed to the line width. Power saturation was present at low pressures although the rf power level was comparatively low, corresponding usually to values of the rectified crystal current ranging between 5 and 12 microamperes. The response time of the recording circuits was not quite negligible for the sweep speeds which were employed. The Stark voltage was not perfectly zero based. During the "off" part of the cycle, the outermost ($m = \pm 3$) Stark component was shifted from 5 to 20 kc/sec.

The observed effects were independent of a reasonable variation of Stark voltage. During the "on" portion of the cycle, the innermost ($m = \pm 1$) component was at least 500 kc/sec away. Theoretically this component should have given well resolved deflection of opposite sign and in size about 1/14 that of the unsplit line. In some recordings, there was some evidence of such a deflection; in others there was not. The fact that this deflection was not definitely observed is to be attributed mainly the narrow bandwidth of the rf system. Also the failure to observe this component may be partly due to the variation of the Stark voltage during the "on" portion of the cycle, this variation causing a broadening of the component. (In Fig. 13 the computed position is 950 kc/sec to the left of the peak. The markers are at 100 kc/sec intervals.)

The recording shown in Fig. 13 is not typical in one respect. Most recordings appeared somewhat asymmetrical. The sign of the asymmetry could be changed by retuning the rf system. Some

calculations were made of line shapes to be expected under a variation of tuning with the measured bandwidth of the rf system of 4 Mc/sec. The observed effects were not inconsistent with these calculations. The calculations also showed that in the extreme asymmetry which could be expected the ratio of one-tenth power line width to one-half power line width might increase from the theoretical value of 3.0 to as large as 3.6. However, the effect of the finite bandwidth of the rf system should be most apparent at high pressures, while the observed increase of this ratio occurred at low pressures. Therefore the major effects which have been reported are not attributable to imperfections in the rf system. However, some residual effects of the finite rf bandwidth might tend to make the value of eQq of 272 kc/sec to be too large rather than too small.

B. Bromoform

1. Introduction

The bromoform molecule has already been investigated in the same frequency region in which we are working. Kojima et al.[28] have reported a large number of lines observed in the region 2400-2600 Mc/sec attributed to the hyperfine structure of the rotational transition J = 0 to J = 1. In addition, Williams and Gordy[29] have studied high rotational transitions in the K-band region. The rotational constants obtained by these two groups of workers, as given here in Table VII, are in serious disagreement.

Table VII

The Rotational Constants of Bromoform

Isotopic Species	B (Mc/sec) (Kojima et al.)	B (Mc/sec) (Williams and Gordy)
$CHBr_3^{79}$	1281	1247.61 ± 0.025
$CHBr_2^{79}Br^{81}$	1270	----------
$CHBr^{79}Br_2^{81}$	1260	----------
$CHBr_3^{81}$	1249	1217.30 ± 0.025

The discrepancy between these sets of measurements is appreciable and cannot be explained by centrifugal distortion alone. As the results of Williams and Gordy are based on the measurement of four different transitions and are given to a great accuracy we were led to assume that the values obtained by Kojima et al. were incorrect. Several considerations involving their experimental procedure also strengthened this belief. The technique used employed no modulation in the detection of lines. A gas sample had to be admitted and pumped out of the absorption cell for each measurement, and the absorption lines were obtained by comparing oscilloscope traces with and without bromoform gas. Compensation for variations in rf power was made by the use of a double crystal circuit. The authors quote a calculated minimum detectable absorption coefficient of 6×10^{-8} cm^{-1}. They calculate the intensity of a representative line as 2×10^{-8} cm^{-1}, while our own estimate is a factor of 5 smaller. It seems difficult to believe that with the slow pumping speed of a heavy gas like bromoform and with the resulting long time interval

between comparative observations lines with such a low signal-to-noise ratio could have been detected.

The object of our work is to obtain the fine structure spectrum belonging to the rotational transition J = 0 to J = 1, using our Stark-modulated spectrograph having a sensitivity of 2×10^{-10} cm^{-1}. From this spectrum it should be possible to evaluate more accurately the rotational constants and also calculate the nuclear quadrupole coupling constants of the two bromine isotopes.

2. Theory

Natural bromine consists primarily of almost equal parts of the two isotopes Br^{79} and Br^{81}. This gives rise to four isotopic species of bromoform, namely $CHBr_3^{79}$, $CHBr_2^{79}Br^{81}$, $CHBr^{79}Br_2^{81}$, and $CHBr_3^{81}$, the relative abundance of which will be approximately one, three, three and one respectively. $CHBr_3^{79}$ and $CHBr_3^{81}$ are symmetric tops and their spectrum is relatively simpler to treat. Both Br^{79} and Br^{81} have a nuclear spin of 3/2. For J = 0 there is no splitting due to quadrupole interaction, but there is splitting due to the inversion doubling of the ground vibrational state. For J = 1 we obtain a number of levels due to quadrupole splitting which depend on the total nuclear spin quantum number I and the total resultant angular momentum quantum number F. The effect of the symmetry introduced by the presence of identical nuclei is to produce two groups of energy levels belonging to the vibrational ground states belonging to the representations A_1 and A_2. A general theory of this type of fine structure is given by Mizushima and Ito[30] who calculated the expected

splitting in terms of the quadrupole coupling constant eQq, resulting in nine lines in the A_1 and three in the A_2 representations. The existence of a low energy degenerate vibrational state gives rise to two more levels belonging to the E representation. In the mixed isotopic molecules the situation is much more complicated and a larger number of lines is predicted.

The Stark effect in this molecule was calculated by us for the various possible values of I and F. Using a formula obtained by Mizushima[31], we found that the maximum Stark splitting at 1000 volts for most of our lines was of the order of 5 Mc/sec, a value adequate for the purpose of resolution.

3. Results

A search for bromoform lines was made in a frequency region ranging from 2240 to 2700 Mc/sec. A large number of lines was found, and these are listed in Table VIII. The lines were investigated with respect to their sensitivity to pressure and to changes in Stark voltage. It was found that the lines could not be made to disappear by continuous pumping of the gas out of the system nor, as a rule, did they show appreciable reduction in size or width. We therefore have no direct proof that the lines do in fact originate in bromoform. The weak response to changes in pressure can be partially explained by the slow pumping speed of this very heavy gas and to the large adsorption on the walls of the cell.

Table VIII

Observed Lines with Bromoform Sample

Line Frequency (Mc/sec)	Intensity	Sensitivity to Pressure	Sensitivity to Stark Voltage	Effect of Dry Ice
2243	3	Strong	Strong	
2265	3	Strong	Strong	
2275	3	Strong	Strong	
2375	2	None	Strong	
2394	3	None	Strong	
2412	1	None	Strong	
2438	4	Some	Weak	
2449	3	Some	Weak	
2457	2	None	Weak	Weaker
2479	5	Strong	Strong	
2506	3	Strong	Strong	Disappears
2525	3	Weak	Weak	Disappears
2549	4	Weak	Weak	Disappears
2565	1			Stays
2606	3			Stays
2612	1			
2649	1			Stays
2684	1			Disappears

This table lists the observed lines attributed to bromoform. The intensities are according to an empirical scale going from 1 to 5. Also listed are the sensitivity of line intensities and shapes to changes in the pressure and in the value of the modulating Stark voltage. In some lines the effect of cooling the cell to dry ice temperature is also listed.

Several lines have already been rejected as spurious, and we suspect that several of those contained in Table VIII will be rejected after further investigations. Essentially all of these measurements have employed the 10' absorption cell with teflon insulation. However, a few days before this portion of the report received its final revision (January, 1954), a few measurements were made using the 20' cell with polystyrene insulation. Several lines failed to reproduce, and it appears that the teflon may be responsible, directly or indirectly, for the inclusion of spurious lines in Table VIII, but this assumption requires further work for confirmation. The ultimate success of the experiment will depend upon obtaining resolution of the Stark splittings of several lines, not only for distinguishing genuine lines from spurious ones but also for identifying particular lines. Because of the complexity of the spectrum, identification of lines appears impossible unless some of them have resolved Stark splittings. While considerable effort has been devoted to attempts at resolving some Stark splittings, no results have been obtained as yet, but there is every reason to expect success in the future.

While some of our lines may be spurious, there is no reason to believe that genuine bromoform lines should escape detection, as the sensitivity of the instrument is adequate. Therefore we can assume that at least some of the lines in Table VIII are genuine bromoform lines. Furthermore, the spectrum reported by Kojima et al., if genuine, should have been discernible. The fact that there

is little semblance between the frequencies of their observed lines and ours seems to indicate that ultimately we shall not be able to confirm their results.

C. The Pure Quadrupole Spectrum of Methyl Iodide Vapor

1. Theory

The conventional method for studying nuclear quadrupole interactions in a molecule is to study the hyperfine splittings of rotational transitions. In fact the preceeding pages contain accounts of our applications of this method to the study of HDO and bromoform.

Another possible method is to observe transitions between quadrupole hyperfine levels without any change in the rotational quantum numbers ($\Delta J = 0$). These transitions logically can be called "pure quadrupole" transitions. With molecules having large quadrupole coupling constants the observation of such transitions is to be considered as a practical possibility, since the lines could have intensities sufficient for observation.

The observation of these quadrupole transitions might permit more accurate determinations of hyperfine splittings than may be possible with rotational transitions. Furthermore it may be possible to obtain information concerning the splittings of very high rotational levels whose rotational transitions are beyond the accessible microwave range.

For the case of a symmetric-top molecule with a single nucleus with quadrupole coupling, the energy levels are given by[32, 33]

$$E = (eQq)\left\{ \frac{3K^2}{J(J+1)} - 1 \right\} Y,$$

where

J = rotational momentum quantum number of molecule,

K = projection of J on molecular symmetry axis,

q = second partial derivative of the potential at the nucleus along the symmetry axis,

Q = electric quadrupole moment,

e = electronic charge.

Y is given by Eq. (5). eQq is referred to as the nuclear quadrupole coupling constant.

This theory has been extended to second order for linear and symmetric-top molecules by Bardeen and Townes[34]. The equation for the energy levels is rather lengthy, and will not be quoted here.

The most favorable opportunity for observing pure quadrupole transitions is when these are accompanied by a change in some property of the electric dipole moment. By reference to Fig. 15 it may be seen when a transition of this type can occur in a symmetric top molecule. The electric dipole moment p is assumed to be parallel to the figure axis and therefore is in the same direction as K. Both p and K precess rapidly about the total rotational angular momentum

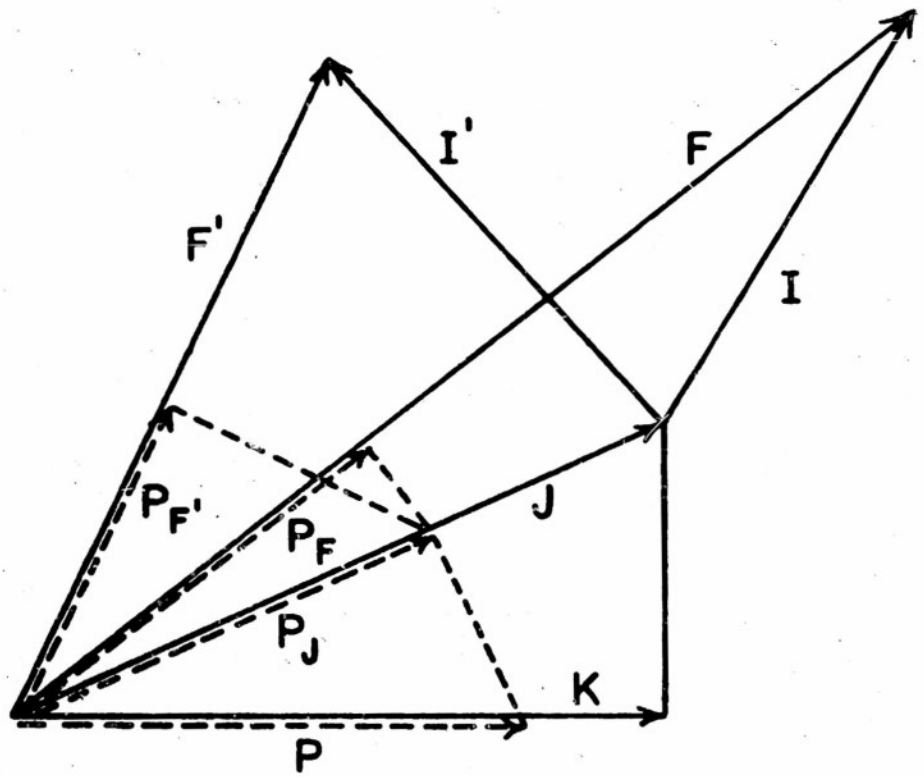

FIG. 15 Diagram of Angular Momentum in a Symmetrical Top Molecule

vector J. The component of dipole moment perpendicular to J averages to zero in time while p_J, the component parallel to J remains constant. J and the nuclear spin I combine vectorially to form the resultant angular momentum F. J and p_J precess around F, the component of p_J perpendicular to F averages to zero, while p_F, the parallel component remains constant. In a quadrupole transition J and I remain constant in magnitude but the angle between them changes giving rise to a new resultant F' and at the same time causing the constant component of electric dipole moment to change to $p_{F'}$. For an interaction of the electric dipole moment with radiation, p_F must be finite for at least one of the two states. When K = 0, this condition is not fulfilled, since p is perpendicular to J, and therefore such an interaction can not occur. However, if K is not zero, such an interaction can occur. It is apparent from this discussion that the biggest changes in p_F occur when it is nearly parallel to J, that is for K = J. Quantummechanical calculations of the proper dipole matrix elements confirm this conclusion.

In a ground vibrational state a linear molecule is the equivalent to a symmetric top molecule in a state for which K = 0. From the foregoing discussion, it is evident that there is no possibility of interaction of the electric dipole moment with radiation. On the other hand if exited into a degenerate bending mode of vibration, such a molecule becomes the equivalent of a symmetric top molecule with $K \neq 0$, and there appears to be a possibility of such an interaction.

2. Calculations on Methyl Iodide

Methyl iodide was chosen for our experiments on pure quadrupole spectra because it is a simple symmetric top molecule with a large quadrupole coupling constant of - 1934 Mc[35] and a relatively large dipole moment (p = 1.647 Debye units). The calculated frequencies and intensities of some of the stronger lines of CH_3I are given below in table IX. In calculating the line intensities the half width of the lines at half maximum has been taken as 20 MC at 1 mm of mercury.

Table IX

Calculated Frequencies and Intensities of Some of the Stronger Lines of CH_3I^{127}

J = K	Transition of F	Calculated Frequency (Mc/sec)	Calculated Intensity (cm^{-1})
1	3/2 → 5/2	292.39	2.8×10^{-10}
2	9/2 → 7/2	374.99	3.7×10^{-10}
3	11/2 → 9/2	444.76*	8.3×10^{-10}
3	3/2 → 5/2	282.53	4.1×10^{-10}
4	13/2 → 11/2	481.10*	3.2×10^{-10}
5	15/2 → 13/2	502.95*	3.4×10^{-10}
6	17/2 → 15/2	517.31	3.5×10^{-10}

* These lines have been observed since this report went to press. The experiment will be reported at the meeting of the American Physical Society, Detroit and Ann Arbor, Michigan, March 18-20, 1954.

ACKNOWLEDGMENTS

We wish to thank Professor W.M.P. Strandberg and Dr. D.W. Posener of M.I.T. for helpful discussions concerning HDO and for access to their results prior to publication. Also we wish to thank Professor C.H. Townes and Mr. R.L. White of Columbia University for helpful discussions concerning quadrupole splittings.

Several important pieces of equipment were obtained from the Western Electric Company through their College Gift Program.

We wish to thank Messrs. Leon Arnell, Leonard Yarmus, and Sol Krongelb for help in constructing the apparatus and to Mr. Howard Greenberg for performing some of the calculations.

Some of the time devoted to the preparation of this report by one of the authors (S.W.) was after he had left New York University and had become a member of the staff of the Bell Telephone Laboratories, Murray Hill, New Jersey. Another author (F.S.) was simultaneously on the teaching staff of the Newark College of Engineering while participating in this work.

REFERENCES

1. H. Lyons, Phys. Rev. 76, 161 (1949). Nuckolls, Rueger, and Lyons, Phys. Rev. 89, 1101 (1953)

2. Kojima, Tsukada, Hagiwara, Mizushima, and Ito, J. Chem. Phys. 20, 804 (1952).

3. L.M. Belleville, M.I.T. Radiation Laboratory Drawing No. D-13633-A, dated 3/26/45. This power supply esentially is the same as that familiarly called an "Oregon" power supply.

4. Lee, Fabricand, Carlson, and Rabi, Phys. Rev. 91, 1395 (1953).

5. Brookhaven National Laboratory Drawing No. P41-13-1-3A, dated 8/25/49. This drawing cites R.E. Hillger of M.I.T. as the original designer of the circuit.

6. R. Beringer, M.I.T. Radiation Laboratory Drawing No. 14292-A, dated 6/16/45.

7. W. Gordy, Rev. Mod. Phys. 20, 668 (1948).

8. C.H. Townes and S. Geschwind, J. Appl. Phys. 19, 795 (1948).

9. C.H. Townes and F.R. Merritt, Phys. Rev. 70, 558 (1946).

10. W.M.P. Strandberg, J. Chem. Phys. 17, 901 (1949).

11. King, Hainer, and Cross, Phys. Rev. 71, 433 (1947).

12. Weisbaum, Beers, and Herrmann, Phys. Rev. 90, 338 (1953).

13. Y. Beers and S. Weisbaum, Phys. Rev. 91, 1014 (1953).

14. Weisbaum, Beers, and Herrmann, "A Preliminary Report on the S+Band Spectrum of HDO", Technical Report No. 195.1 of this project.

15. W.S. Benedict, Private Communication.

16. King, Hainer, and Cross, J. Chem. Phys. 11, 27 (1943).

17. D. Kivelson and E.B. Wilson, J. Chem. Phys. 20, 901 (1952).

18. D.W. Posener and W.M.P. Strandberg, J. Chem. Phys. 21, 1401 (1953).

19. Jen, Bianco, and Massey, J. Chem. Phys. 21, 520 (1953).

20. R.E. Hillger and M.W.P. Strandberg, Phys. Rev. 83, 575 (1951).

21. Benedict, Gailar, and Plyler, J. Chem. Phys. 21, 1302 (1953).

22. See for example, H.E. White, "Introduction to Atomic Spectra", McGraw - Hill Book Company, Inc., New York (1934), p. 206 and Table III, p. 439. Here J, L, and S are replaced respectively by F, J, and I.

23. R. L. Carter and W.V. Smith, Phys. Rev. 73, 1053 (1948).

24. J.K. Bragg, Phys. Rev. 74, 533 (1948).

25. King, Hainer, and Cross, J. Chem. Phys., 12, 210 (1944).

26. R.L. White, Phys. Rev. 91, 1014 (1953).

27. S. Geschwind, Annals of the New York Academy of Sciences, 55, 751 (1952).

28. Kojima, Tsukada, Hagiwara, Mizushima, and Ito, J. Chem. Phys. 20, 804 (1952).

29. Q. Williams and W. Gordy, J. Chem. Phys. 20, 1524 (1952).

30. M. Mizushima and T. Ito, J. Chem. Phys. 19, 739 (1951).

31. M. Mizushima, J. Chem. Phys. 21, 539 (1953).

32. D.K. Coles and W.E. Good, Phys. Rev. 70, 979 (1946).

33. J.H. Van Vleck, Phys. Rev. 71, 466 (1947).

34. J. Bardeen and C.H. Townes, Phys. Rev. 73, 627 and 1204 (1948).

35. Gordy, Simmons, and Smith, Phys. Rev. 74, 243 (1948).